LUNDS
UNIVERSITET

Development of an *in vitro* assay for analysis of cellular uptake of nanoparticles

Lina Olsson

Masters degree in molecular biology
Examensarbete i molekylärbiologi 30 hp till masterexamen 2013
Spago Imaging AB and
Department of Biology, Lunds University

Table of Contents

Abbreviations

APTMS = 3-aminopropyltrimethoxysilane

AuNP = gold nanoparticles

CT = computed tomography

DLS = dynamic light scattering

DMEM = Dulbecco's modified Eagle medium

EPR = enhanced permeability and retention

FBS = fetal bovine serum

ICP-AES = inductively coupled plasma atomic emission spectroscopy

IXG-P = Ion-X-Gel precursor

MRI = magnetic resonance imaging

NMR= nuclear magnetic resonance

NP= nanoparticle

NSF = nephrogenic systemic fibrosis

PBS = phosphate buffered saline

PEG = poly ethylene glycol

PET = positron emission tomography

RES = reticuloendothelial system

RPMI-1640 = Roswell Park Memorial Institute medium type 1640

SPIO = superparamagnetic iron oxide

Acknowledgements

I would like to express my deep gratitude to my supervisor Emil Aaltonen at Spago Imaging AB for his patient guidance, enthusiastic encouragement, his providence of useful critiques of my research work and above all his willingness to give me his time during the project. My grateful thanks and appreciation are extended to all members at SPAGO Imaging AB for all help and knowledge provided for me during the project and for giving me the possibility to do the thesis at SPAGO Imaging. I very much appreciate all the knowledge and experience I have gained during this time.

Abstract

MRI, magnetic resonance imaging, is used for disease detection such as assessing blood flow, detecting tumours and diagnosing many forms of cancer. Contrast agents are chemical substances that increase the MRI sensitivity. One class of contrast agents are the so called nanoparticulate contrast agents. Since tumour-associated formation of new blood vessels often results in highly permeable vessels, appropriately sized nanoparticles can selectively leak from the blood flow into the tumour interstitium and accumulate in tumours. This creates an increased difference in contrast between normal and abnormal tissue in an image.

Spago Imaging AB is developing a novel and tumour specific nanoparticle based contrast agent. In solving the clinical evaluation of the nanoparticle it is important to know how the nanoparticle interacts with specific cells and tissues types. In this thesis work, an *in vitro* based assay was developed so that one aspect of the nanoparticle cell interactions can be studied; cellular uptake.

The assay was developed using three reference particles, PEGylated gold nanoparticles and Superparamagnetic iron oxide nanoparticles (SPIO) which were in this study successfully functionalized with PEG1000 and APTMS. All three are known from literature to be internalized in certain cell lines [1-3]. HepG2 hepatocytes cells and human breast carcinoma cells MDA-MB-231 cells were used as models. By investigating the effect of cell density and amount, exposure time, nanoparticle concentration and particle surface characteristics, a functional assay could be set up. ICP-AES analysis and T_1 and T_2 relaxivity measurments showed that the internalization of nanoparticles occurred in a concentration dependant manner. The assay was used to test cellular uptake of a precursor of Spago Imaging AB Ion-X-gel, itself a staring material for the final contrast agent product. The findings indicated that the Ion-X-Gel precursor was internalized in a concentration dependent manner. The study also demonstrated that silane-coated SPIO nanoparticles possessed a higher *in vitro* labeling efficiency in HepG2 cells compared to PEG coated SPIO nanoparticles.

The results will give a better understanding of how the nanoparticles behave in a biological system and can in the long run help the developmental process to produce a product with the potential to provide more accurate diagnosis, earlier detection of tumours, a decrease in the number of false positives and above all, it could lead to less suffering for patients.

1. Introduction

Every day, people of all ages all over the world are diagnosed with cancer. Early detection of tumours is important as it increases the chances for a correct and successful treatment meaning the possibility for full recovery is much greater. But this has proven to be a challenge as current methods for tumour imaging varies in effectiveness and are not of sufficiently high quality to meet all aspects necessary for accurate tumour visualization. Mammography is fast and cheap but is lacking in sensitivity, i.e. not finding all tumours [4]. Mammography, as well as computed tomography (CT) and positron emission tomography (PET), use ionizing radiation which increases the risk of cancer. These traditional diagnostic methods can all be harmful to normal cells and can damage healthy tissue [5].

MRI is a non-invasive and quantitative method for imaging, and is considered to have a higher sensitivity compared to other alternatives. The downside with MRI is that it suffers from a high number of false positives [6]. Development of supplements that can increase the capabilities of the imaging tools used today is therefore important. Nanomaterials are such supplements. Nanoparticles as contrast agents enhance the contrast of structures within the body which allows for distinguish normal tissue from abnormal conditions in images. Spago Imaging AB is developing a novel and tumour specific nanoparticle (NP) based contrast agent to be used in MRI. It is necessary to gain understanding of if and how the particles are internalized and transported within the cells, and to which extent they are metabolized and excreted. The toxicity of nanoparticles *in vivo* is a concern as they can be cleared from circulation and accumulate in the spleen, liver or bone marrow. In order to gain knowledge of such events, *in vitro* studies of interactions between nanoparticles and various cell types with respect to cellular uptake is important as this could enable greater control over internalization of nanoparticles by the cells and thus perhaps limiting toxic effects, and increasing the desired effects.

1.1. Aims

The aim of this master thesis work was to develop and set up an *in vitro* based assay which can be used to study cellular uptake of nanoparticles. The assay is meant to be used to analyse cellular uptake of Spago Imagings Ion-X-gel precursor (IXG-P) and other nanoparticle based products. The uptake of IXG-P was expected to be low and a reference particle was therefore important to include in the experiments in order to confirm the function of the set up. Parameters such as cell density, nanoparticle concentration, exposure times, particle surface characteristics and different reference nanoparticles were to be tested as to find optimal assay conditions.

1.2. Magnetic resonance imaging (MRI)

MRI uses a combination of magnetism, radio waves with different frequencies and a computer to produce images of body structures and organs. It is used for disease detection such as assessing blood flow, evaluating infections, assessing injuries to bones and joints, detecting tumours and diagnosing many forms of cancer [7]. MRI is based on the principles of nuclear magnetic resonance, NMR, a spectroscopic technique to obtain chemical and physical information about molecules where the interactions between atomic nuclei and their behaviour in a magnetic field are observed. A property of atomic nuclei is the intrinsic spin angular momentum which is the spinning of the nuclear particles around an axis at a constant rate or velocity [8].

The body consists of mostly fat and water which both contain hydrogen. Since ^1H is the most abundant isotope of hydrogen, it is the natural choice for probing the body using MRI. All hydrogen protons have spin vectors of equal magnitude but with different spin orientations. When a magnetic field is applied, the net magnetization vector lies along the direction of the magnetic field and is called the equilibrium magnetization. By exposing the nuclear spin system to short pulses of radio pulses containing many frequencies spread over a narrow range, the net magnetization can be changed. The inversion recovery pulse sequence results in 180° rotation of the net magnetization along the Z axis after application of a pulse. A second pulse of 90° tilts the Z-magnetization into the XY-plane (see Figure 1).

T_1 is related to the time it takes for the net magnetization to return to its equilibrium position along the Z axis and is called spin lattice relaxation time [8]. T_2 is the time it takes for the transverse magnetization in the XY plane to return to equilibrium (no spin in XY-plane) and is called the spin-spin relaxation time. T_2 relaxation emits energy and the signal is proportional to the population difference between the states [9].

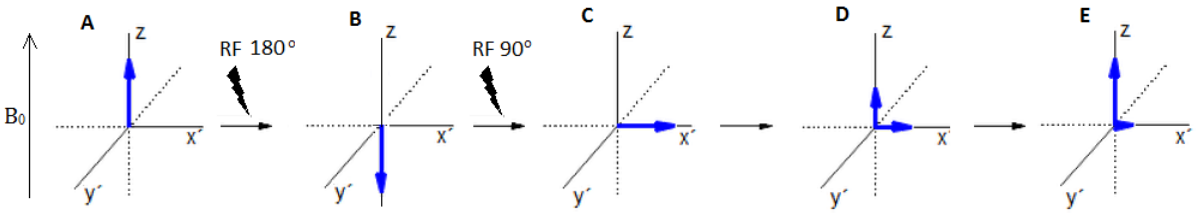

Figure 1. The effect on spin vectors when pulses in the form of radiofrequencies are applied. A) The sample is placed in a magnetic field (B_0) and magnetization equilibrium along the Z-axis is established. B) 180° pulse is applied resulting in inversion of net magnetization. C) 90° pulse is applied resulting in tilting of net magnetization. D and E) The magnetization is gradually returned to equilibrium.

Determination of where in the body the energy is being released is achieved by placing magnetic field gradients on the body. This enables the computer to generate a two- or three-dimensional map. The amount of magnetisation depends on the strength of the external magnetic field so higher field strength usually allows for more detail within the image [10]. T_1 and T_2 are both tissue-specific and MRI is based on difference in the T_1 and/or T_2 relaxation times of tissues [10]. Diseased or damaged tissue display

differences in T_1 or T_2 compared to normal tissue. Despite the variance in T_1 and T_2 relaxation times between tissues, the difference is often not high enough for detailed imaging. Thus for this reason, a MRI contrast agent is often introduced to increase the signal difference between normal and pathological tissue [9].

1.3. Contrast agents

Contrast agents used in MRI will not themselves generate any signal. Instead they act as indirect agents by affecting the T_1 and/or T_2 relaxation times of the water protons in the proximity of the contrast agents. Each tissue is characterised by a relaxation time T_1. If T_1 is shortened the time between the applied consecutive 90° RF pulses can be cut down which results in enhanced differences between the longitudinal recoveries between tissues with different T_1 and thereby MRI sensitivity is increased.

Many kinds of contrast agents are available, e.g. molecules containing gadolinium, manganese, cobalt, nickel and iron. Contrast agents can be grouped as either positive or negative. In general, positive contrast agents cause a reduction in T_1 relaxation time. In an MRI image this shows as a whiter area compared to the surrounding tissue. Positive contrast agents are often small molecular weight compounds containing gadolinium or manganese. Negative agents result in shorter T_1 and T_2 relaxation times but with a much larger effect on T2. In an MRI image this shows as a darker area compared to the surrounding tissue. Examples of negative agents are those based on SPIO, which was used in this study.

The most commonly used compounds for contrast enhancement are gadolinium-based [11]. Severe side effects of gadolinium can be seen in patients with renal insufficiency or dysfunction with risk of developing nephrogenic systemic fibrosis (NSF) [12]. NSF results in the fibrosis of soft and connective tissue [13] and it is progressive and may be debilitating or fatal. The gadolinium based chelates can rapidly distribute in the body leading to a short time-window for imaging and low contrast between tumour and surrounding tissue and limit correct diagnosis [14].

1.4. Enhanced permeability and retention effect

Contrary to healthy tissue, many tumours possess several unique pathophysiological and anatomical characteristics which results in something collectively known as the enhanced permeability and retention (EPR) effect. The most important characteristic is a high density but defective vascular architecture due to extensive angiogenesis and an increased production of a number of permeability mediators which leads to large gaps between endothelial cells in tumour blood vessels. An impaired lymphatic drainage/recovery system is also characteristic which provides a selective extravasation and retention of macromolecular drugs [15]. This EPR effect serves as a base for anticancer therapy and nanoparticle based contrast imaging as nanoparticles extravasate from the leaky tumour vasculature to a higher degree than healthy

vasculature, and remain in the tumour area. This results in a concentration difference of the nanoparticles in tumour tissue compared to normal tissue [16].

1.5. Nanoparticles

One class of contrast agents are the nanoparticle contrast agent where the magnetic properties and toxicity are two of the most important parameters in the design [16]. Nanoparticles are smaller than cells but larger than many proteins with sizes ranging from one to hundreds of nanometres. The particles take advantage of the unique abnormalities of the tumour tissue, such as the EPR effect, to reach their target sites.

Physiological environments such as cellular cytoplasm, blood and interstitial fluid contain a mixture of proteins, ions and molecules each of which may potentially interact with a nanomaterial. Nanoparticles can, when exposed to proteins, ions and molecules aggregate as these can rapidly adsorb to the nanoparticles surface. Aggregation of nanomaterials can affect the degree of toxicity and cellular uptake depending on the nanoparticles composition and the cell type [17]. *In vivo* toxicity of nanoparticles is a concern as nanoparticles can be shuttled out of circulation and accumulate in the spleen, liver or bone marrow via uptake by the reticuloendothelial system (RES) [1].

Ion-X-gel Precursor (IXG-P)

Spago Imaging AB is developing a tumour specific nanoparticle based contrast agent. As a platform for the development, particles named Ion-X-gel (IXG) are used. The gadolinium free IXG particles consist of cross-linked polar polymers and manganese and the resulting product has exceptionally high relaxivity. Manganese chelates are T_1-shortening contrast agent. Due to low toxicity and high relaxivity, manganese-based contrast agents display favourable properties in MRI diagnostics compared to gadolinium which is more toxic than Mn^{2+} [18]. The size of IXG (5nm) is highly compatible with passive tumour targeting (EPR) which makes the particle accumulate in the tumour tissue and be excluded by healthy tissue. One important aspect in the development of the particle is to study how the nanoparticles interact with biological systems. Of specific interest is to understand how they interact with living cells originating from various tissues. Such knowledge allows for further development of the particles with respect to e.g. excretion from the body, limiting the interaction with non-tumorous tissue and increasing tumour targeting. IXG-P nanoparticles are the precursors for Ion-X-gel nanoparticles. IXG-P does not contain manganese and is partially composed of silicon.

Superparamagnetic iron oxide (SPIO)

SPIO are magnetic nanoparticle probes and they are widely utilized in biomedical applications, such as *in vitro* studies of nanoparticle uptake by cells**.** Both the T_1 and T_2 relaxation times are shortened by SPIO, but the changes induced are dependent on the size of the particle, their size distribution, their coating and if they act extracellularly or

intracellularly [16]. SPIO have been shown to have a minimal impact on cell viability and function [19]. SPIO show a more extensive shortening of T_1 and T_2 relaxation times in comparison with gadolinium containing chelates [16].

SPIO that are used in biochemical applications are most commonly surface modified with hydrophilic agents that are coated on the surface to prevent nanoparticle aggregation, reduce toxicity and to control pharmacokinetics and biodistribution [19]. When administered by intravenous injection, SPIO is predominantly cleared from circulation by macrophages, that reside in organs rich in reticuloendothelial cells [20]. In general, SPIOs are internalized by receptor-mediated endocytosis and are metabolized via the lysosomal pathway [20]**.** Iron oxide is biodegradable, and the iron from degraded SPIO particles is incorporated into the body's iron store and is progressively found in haemoglobin, the iron-containing protein in the red blood cells [20]. SPIO was used for structuring the assay in this study as previous publication indicated that SPIO was internalized by cells [21].

Gold nanoparticles (AuNP)

The SPIOs used in this work were larger (70nm) and not of the same size range as the IXG-P (5 nm). Therefore a second type of molecule consisting of gold nanoparticles, in the same size range as IXG-P, was evaluated to be used as a positive control.

Inorganic gold nanoconstructs are used in experimental targeted cancer therapy. They are the most stable and popular nanoparticles as they can be synthesized with very precise sizes, shapes and surface chemistries using relatively simple chemistry [22]. Plain gold nanoparticles have been shown to aggregate under physiological conditions whereas coating the AuNP with PEG has been shown to increase the stability of the particle [23]. Cellular uptake of gold nanoparticles is size dependent and particles with a smaller core diameter (30-50 nm) has been shown to be taken up by the cells to a higher extent compared to larger particles [23].

1.6. Coating

Limitations of the use of nanoparticles are still in the process of being solved. To prevent concerns such as nonspecific binding to nontargeted or nondiseased areas, toxicity of the particles on its pathway through the body as they are oxidized and degraded [16] and aggregation of the particle, molecules can be covalently attached or adsorbed onto the surface of the nanoparticles in a process called coating. The coating shields the nanoparticles and extends the time of circulation of the particulates from minutes to hours, thereby increasing the tumour targeting efficiency of a nanoparticles formulation capabilities [24]. Examples of coating molecules include dextran, carboxymethylated dextran, starches, poly ethylene glycol (PEG) and DNA [16]. The specificity of a particle can be increased when it is correctly coated.

Poly ethylene glycol (PEG)

Some of the concerns regarding nanoparticles aggregation and absorption of plasma proteins is reduced by coating the particles with PEG [17]. PEG was used in this study as a stabilizer of SPIO and AuNP. PEG is a coiled polymer of repeating ethylene ether units with dynamic conformations. It has good water solubility and has the ability to dissolve in organic solvents. The PEG chains reduce interactions by increasing the steric distance between them and by increasing hydrophilicity by the hydrophilic ethylene glycol repeats. PEGylated NPs generally reduce the accumulation in the liver between 25-50 % of the amount of non-PEGylated NPs. The size of nanoparticle can also be changed with PEG.

It has been shown in previous publications that immobilization of PEG on nanoparticles increases the amount of uptake into cancer cells compared to unmodified nanoparticles [2]. This is the result of solubilisation of the particle in the cell membrane lipid layer mediated by PEG [25, 26].

1.7. Endocytosis

Nanoparticles enter the cell via endocytosis. Endocytosis is a process where invagination of the plasma membrane and formation of intracellular vesicles is seen. This process enables e.g. uptake of extracellular nutrients and entry of viruses and toxins. Phagocytosis and pinocytosis are different types of endocytosis. Phagocytosis involves the uptake of larger particles (>0.25 μm), such as bacteria, while pinocytosis involves the ingestion of particles via small vesicles (<0.2μm).

The rate and mechanism of uptake of nanoparticles is cell-type dependent and varies with nanoparticle size, charge, and other surface properties. It is therefore difficult to draw general conclusions about how to produce particles for maximized or minimized cellular uptake. Reports have shown that nanoparticles in the range of 20–50 nm are taken up more rapidly compared to smaller or larger particles [27, 28].

Endocytosis is mostly studied by using electron microscopy, fluorescently labelled nanoparticles and confocal microscopy. Reports have shown that internalized nanoparticles are found mainly in endosomes or lysosomes [29]. These organelles have low pH, and lysosomes contain proteases and other enzymes that degrade the particles. Exocytosis of nanoparticles has been studied and results indicate that this process is slower compared to endocytosis. The rate of exocytosis decreases with increasing particle size [27, 28].

1.8. Cell culture

Cell culture is a major tool used in cellular and molecular biology. Due to the ability of culturing many cells from one batch of cells, results obtained can be reproducible and consistent. It provides systems for studies of toxicity and effects on cells by e.g. drugs

and biological compounds such as vaccines. Cell culture models can be used to e.g. investigate the risk of specific compounds to cause cancer in humans, to study drug metabolism and to monitor changes in the genome or proteome upon various stresses. Cells cultured *in vitro* often grow as monolayer on an artificial substrate that allows for adhesion onto the surface. Cell yield is proportional to the area of the surface where they are allowed to grow.

HepG2

A widely used cell line is the human hepatocellular carcinoma cell line HepG2. The cells are immortal polarized hepatocytes from the liver tissue of a fifteen year old male with differentiated hepatocellular carcinoma. They are epithelial-like cells growing as monolayers and in small aggregates. These cells are highly differentiated and display many of the genotypic features of normal liver cells [30]. Because they share many morphological and functional characteristics with cells from normal liver tissue, HepG2 cells are used for cell-based assays of liver function, metabolism, and compound toxicity. HepG2 was chosen since several publications have shown to internalize SPIO nanoparticles [2, 31].

MDA-MB-231

The cell line MDA-MB231 is a human breast carcinoma cell line with epithelial cell morphology and they grow in monolayer. It was derived in 1973 from a Caucasian 51 year old woman who had received no radiotherapy. MDA-MB-231 cells were chosen as they have been shown to internalize SPIO nanoparticles to a lower degree compared to HepG2 cells [2].

1.9. Methods for analysis

Concentration determination of iron, silicon and gold was done with inductively coupled plasma-atomic emission spectrometry (ICP-AES) and UV spectrophotometry. Determination of T_1 and T_2 was done using a bench top NMR analyser. Dynamic light scattering (DLS) was used to characterize the size of the different particles. For determination of cell , two dose-response tests were used together with an absorbance micro plate reader and a fluorescence microplate reader.

ICP-AES

ICP-AES uses the fact that as excited electrons returns to ground state they emit electromagnetic radiation at a given wavelength. Each element emits energy at specific wavelengths. The intensity of the energy emitted at the chosen wavelength is proportional to the amount of that element in the analysed sample.

As the sample solution is placed into a ICP-AES it is pumped into a so called nebulizer where it becomes atomized into an aerosol mist. The droplets of the mist are injected with a stream of argon gas into ionized argon plasma. The plasma contains free

electrons and charged ions and the liquid droplets become ionized and are converted to salt particles. The salt particles are separated into molecules and will fall apart to atoms and ions. More energy is transferred to the atoms and ions and this procedure excites the valence-electrons of the elements in the sample. When the electrons return to their ground state at a certain position in the plasma, the relaxation emits electromagnetic radiation. The intensity of the radiation is proportional to the concentrations of the element, thus calculations can be done to obtain the exact amount of the element that is present in the solution.

Relaxometry

A bench top NMR analyser was used for T_1 and T_2 measurments. NMR makes use of the nuclei in substances as sensors of their surroundings. It is a contactless and non-destructive analytical method as both excitation and detection are performed via electromagnetic waves in the radiofrequency region.

Dynamic light scattering (DLS)

DLS can be used to measure particle/molecular size, absolute molecular weight and zeta potential in the size region as low as below 1 nm. The system was used to measure the size of nanoparticles. It measures the Brownian motion of particles, which is the movement of particles due to random collisions with molecules of solvent. When illuminating the particles with a laser light source, the particles scatter the light with different intensities in all directions, known as Rayleigh scattering. The intensity fluctuations are analysed and the system measures the rate of intensity fluctuation and can from this data calculate the size of the particle [32].

Dose-response assessment

CellTiter AqueousOne

For assaying dose-response a colorimetric method was used, named CellTiter 96® Aqueous One Solution Cell Proliferation Assay. The solution regent contains a tetrazolium compound which is bioreduced by cells into a coloured formazan product that is soluble in tissue culture medium. The conversion into the coloured formazan is thought to be accomplished by NADH or NADPH that is being produced in metabolically active cells. The quantity of formazan product as measured by the absorbance at 490 nm is directly proportional to the number of living cells in culture.

An absorbance micro plate reader was used when dose-response was tested with AqueousOne. It uses a light beam with a specific wavelength to illuminate the samples in a vertical axis within a 96 well plate. A detector placed on the other side of the plate measures the amount of the initial light is being absorbed by the sample. The absorbance is proportional to the concentration of the light absorbing solution in the well.

CellTiter Blue

Due to high standard deviations and fluctuating results using the Aqueous One dose-response test a second test was used; CellTiter-Blue® Cell Viability Assay. The assay is based on the ability of viable, metabolically active cells to reduce a resazurin-based fluorescent compound to resorufin (see Figure 2). This conversion is intracellular as resazurin is metabolized by mitochondrial, microsomal and cytosolic oxidoreductases to resorufin. Resazurin itself is a nonfluorescent blue dye but when reduced to Resorufin it becomes fluorescencent. Resorufin is detected with a fluorimeter at excitation wavelength 560 nm. The mitochondrial activity is proportional to the total amount of cells, and the rate of dye reduction is therefore directly proportional to the number of viable cells present [33].

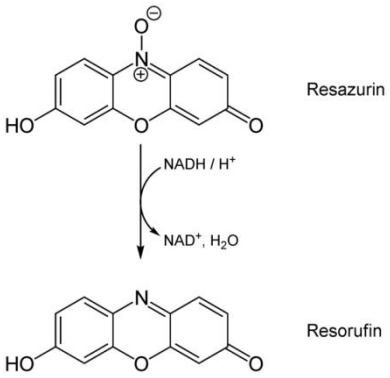

Figure 2. The conversion of Resazurin to Resorufin.

Fluorescence intensity detection has a broader range of applications compared to absorbance detection as it is more sensitive. An optical system illuminates the sample with a specific wavelength and the sample is thereby excited. The sample emits light (fluoresces) and a second optical system (emission system) collects the emitted light, separates it from the excitation light, and measures the signal using a light detector.

2. Materials and methods

2.1. Synthesis and characterization of nanoparticles

SPIO

SPIO particles in an aqueous solution were purchased from Sigma-Aldrich. According to the product specification the SPIO concentration was 5 mg/ml with a particle size of 9-11 nm. These particles will be referred to as A-SPIO.

70 nm SPIO at 7 vol % magnetic iron (II,III) oxide in aqueous solution were purchased from ABCR in Germany. These SPIO will be referred to as naked SPIO.

PEGylation of SPIO

In order to stabilize the nanoparticles, SPIO nanoparticles were mixed with PEG of three different molecular weights. The PEGs used were polyethylene glycol methyl ether (PEG500), poly ethylene glycol (PEG1000) and poly acrylic acid. PEGylation of A-SPIO and naked SPIO was done as follows; SPIO, PEG1000, PEG500 and polyacrylic acid were diluted in water. 0.2 ml SPIO at 0.165 mg/ml was mixed with 0.2 ml 700 µM, 360 µM and 70 µM PEG1000, PEG 500 and polyacrylic acid. The mixtures were incubated overnight at room temperature.

The stability of all PEGylated SPIO was examined by adding particles to H_2O, saline and cell culture medium (DMEM and RPMI) with and without 10% FBS. The solutions were visually examined after 2 h incubation at room temperature. Only naked SPIO coated with PEG1000 ($H(OCH_2CH_2)_nOH$) remained in solution indicating that these particles were stable. The PEGylated SPIO particle will be referred to as P-SPIO.

Previous publications have shown that an elevated temperature (60°C) leads to partial dehydration of PEG molecules, permitting PEG molecules to be packed onto the NP surface with higher density [34]. Therefore, a solution of P-SPIO was heated for 1 h at 60°C. This particle will be referred to as H-SPIO.

Coating of SPIO coated with APTMS

It is known that different coatings can affect cellular uptake. One coating which is known to increase cellular uptake is 3-aminopropyltrimethoxysilane (APTMS) [2].

Thus, naked SPIO were coated with APTMS. The amount of iron atoms that is accessible on the outside of the nanoparticle was estimated to 5% and the mole relationship between silane and surface accessible iron was calculated thereafter.

100 µl naked SPIO was diluted with 900 µl 70% EtOH and the solution was put in a sonication bath for 1 h at 37°C. 2 µl concentrated APTMS was added to the naked SPIO. The mixture was put in an ultrasonic bath for 2 h at 37°C. The EtOH was removed by exposing the nanoparticle solution to a stream of nitrogen gas for 5 min by flushing the

gas through a glass pasteur pipette which was held just above the surface of the solution. The particles were then dried overnight at 50°C for removal of water. The particles were resuspended in 1 ml Milli-Q water and were put in sonication bath for 2 h. The solution was filtered through a 0.2 µm SUPOR syringe membrane (PALL) for removal of aggregates. The particles will be referred to as S-SPIO.

In order to establish the presence of an APTMS coating on the S-SPIO particles, ninhydrin was used according to a pervious publication [35]. When the ninhydrin reacts with amines, a deep blue or purple colour known as Ruhemann's purple is produced. 50 mg ninhydrin was dissolved in 200 µl 99.5% EtOH. The silanized particles were spotted onto a filter paper using glass capillaries and the ninhydrin solution was spotted on top of the spots of silanized particles. As a control, APTMS in 70% EtOH was spotted onto the filter paper and ninhydrin was added on top of the spot.

Gold nanoparticles (AuNP)

PEG coated AuNPs were provided by a co-worker at Spago Imaging AB.

Precursor of Ion-X-gel nanoparticles

The precursor of Spago Imaging Ion-X-gel is a 5 nm polymeric nanoparticle consisting mainly of silicon, phosphorus and carbon. These particles will be referred to as IXG-P.

Size determination of nanoparticles

Size determination of the nanoparticles was done with Dynamic Light Scattering using Zetasizer ZEN3600 from Malvern Instruments. Large particles, such as dust, can scatter light intensely and can interfere with the DLS signal from the particles. Therefore, samples were filtered with GHP Acrodisc 13 mm Syringe filter with 0.2µm GHP membrane (PALL) prior measurements. Filtered samples were measured in capped plastic cuvettes. The machine was programmed for 5 measurement repetitions to ensure that the DLS measurements were reproducible. Water was used as a blank.

2.2. Determination of nanoparticle concentrations

Determination of concentrations of nanoparticle stock solutions

The concentration of iron, gold and silicon in the nanoparticle stock solutions was determined by ICP-AES. IPC analyses were done at Växtekologens Laboratory at the Department of Biology at Lunds University. The P-SPIO, S-SPIO and naked SPIO were sterile filtered with 0.2 µm SUPOR syringe membrane (PALL) and diluted with 12 M HCl to the final concentration of 5 M HCl in order to bring the iron into solution. The detection limit for iron with ICP analysis is 1 ppb (1µg/L). AuNP were dissolved in aqua regia, 12 M HCl and 15 M HNO_3 (ratio 3:1), and were analysed with ICP. The detection limit for gold is 1 ppb (1 µg/L). Silicon content in IXG-P solution was analysed with ICP after the addition of 0.1% HNO_3. The detection limit for silicon is 10 ppb (10 µg/L).

Determination of concentrations of nanoparticles in cell cultures

Iron concentration determination

Determination of iron concentrations in cell cultures were initially done with the thiocyanate method. This method proved to be too insensitive as the obtained values were in the same range as the detection limit. Therefore a more sensitive method based on ferrozine was used. Both methods are described below. However, the ferrozine method was also too insensitive so instead ICP analysis was used for the final experiments. Prior to ICP measurements the cell culture samples were mixed with 12 M HCl to a final concentration of 5 M.

The thiocyanate method

Thiocyanate reacts with Fe^{3+} and forms a red coloured complex, the intensity of which can be measured spectrophotometrically [36]. By using a solution with known concentration of Fe^{3+}, a calibration curve was recorded. Different volumes of 1 mM $FeCl_3 \cdot 6H_2O$ (standard solution) was mixed with 1 M H_2SO_4 and 1 M KSCN in volume ratio 1:50 to the final volume of 1 ml. Absorbance spectra was obtained from measurements on the solutions containing different volumes of the standard solution. Cell-based samples were diluted with 4 M HCl (volume ratio 1:1) and incubated overnight at 60°C, 240 rpm on a shaking table. The samples were centrifuged for 10 minutes at 12000×g in order to remove macroscopic particles. The supernatant was mixed with 1 M KSCN (volume ratio 1:1) and 1 M H_2SO_4 (volume ratio 1:100) and the samples were incubated for 10 min at room temperature. The absorbance of the samples was measured with UV-Spectrophotometer (UV-1800 from Shimadzu) at the absorption maximum determined by the calibration curve and the iron concentration in the samples could be calculated.

The ferrozine method

Ferrozine reacts with Fe^{2+} ions to form a purple-colored complex the intensity of which can be measured spectrophotometrically [37]. 10 standard samples containing different concentrations of Fe^{2+} with water as diluent (total volume 670 µl) were mixed with 100 µl 0.01 M ferrozine, 150 µl 30% $NH_2OH \cdot HCl$ and 80 µl buffer consisting of 5 M CH_3COONH_4 and 4 M KOH (volume ratio 5:3). A calibration curve was obtained using the 10 standard samples. Dilutions of cell based samples were done with 4 M HCl and the samples were heated for 24 h at 60°C at 240 rpm. The samples were centrifuged for 10 min at 12000×g in order to remove macroscopic particles. The supernatant was diluted with 220 µl H_2O + 100 µl 0.01 M ferrozine + 110 µl 4 M KOH + 150 µl 30% $NH_2OH \cdot HCl$. After 10 min, 80 µl 5 M CH_3COONH_4 (adjusted to pH 9.5 with NH_4OH) was added. The absorbance was measured and the iron concentrations were determined.

Gold and Silicon concentration determination

Determination of gold concentrations in cell cultures was done by incubation with aqua regia, 3:1 mixture of 12 M HCl and 15 M HNO_3, in order to bring the nanoparticles into

solution according to a previous publication [38]. Cell cultures were mixed with aqua regia in a volume ratio 2:3. Determination of gold concentrations was done by ICP analysis.

Determination of silicon concentrations in cell cultures was done by incubation with KOH in order to bring the nanoparticles into solution. Cell cultures were mixed with 4 M KOH in a volume ratio 2:3. The basic solution was mixed with 6 M HNO_3 to a final pH of 9. Determination of silicon concentrations were done with ICP analysis.

Relaxivity

Prior to preparing the cell samples for ICP analysis, T_1 and T_2 relaxivity was measured with an NMR analyser, (Minispec mq 60 from Bruker). 200 µl samples were pipetted into NMR glass tubes. For T_1 measurements the following settings were used; 4 scans, pulse separation of 1 ms, recycle delay of 5 sec with duration of 10 sec. For T_2 measurements the following settings were used; 4 scans, pulse separation of 1 ms, 200 data and recycle delay of 20 sec.

2.3. Culturing of MDA-MB-231 and HepG2 cells

The cells in this study were cultivated in single use sterile polystyrene flasks with ventilated caps with surface area of 25 cm^2, 6 well plates, 24 well plates and 96 well plates from Nunclon and 4Titude.

MDA-MB-231 cells were grown in RPMI-1640 with 10% FBS and 100 µg/ml penicillin/streptomycin. HepG2 cells were grown in medium Dulbecco's modified Eagle Medium (DMEM) with 10% FBS and 100 µg/ml Penicillin/Streptomycin. For culture initiation, 10^6 frozen cells were thawed. The cell suspension was then transferred to a 75 ml culturing flask and 11 ml preheated medium was added drop wise to the flask in order for the cells to adjust to the environment.

The cell cultures were split as follows; the cells were viewed with a microscope to confirm a good health status. The medium was aspirated. The cells were washed with 5 ml pre-heated PBS for removal of residual medium. One ml pre-heated 0.05% trypsin solution was added to the cells and the flask was placed in an incubator for 5 minutes. The cells were examined to ensure that they had detached from the bottom of the flask. Nine ml pre heated medium was added and the cell suspension was pipetted over the flask bottom 4 times. Two ml cell suspension was moved to a fresh flask and 10 ml fresh medium was added. The cultures were incubated in an incubator (37 °C, 5% CO_2, 95% humidity) for 3-4 days, where after the procedure was repeated.

2.4. Dose-response assessment

The dose-response was determined using two kits from Promega, CellTiter Aqueous One and CellTiter Blue. Dose-response tests were done on cells grown in 96 well plates. Five

thousand cells per well were seeded. For dose-response tests using CellTiter 96 AqueousOne Solution, 180 µl cell suspension was dispensed into 11 columns of a 96 well plate (Nunclon surface). One column was left empty. For dose-response tests using CellTiter Blue, 90 µl cell suspension was dispensed into 11 columns in a 96 well OptiPlate (4Titude) and one column was left empty. The plates were incubated overnight prior to addition of nanoparticles.

Preparing sample dilutions

Prior to all dose-response tests, the particles and diluents were sterile filtered with 0.2 µm SUPOR membrane syringe filters (PALL). The first dose-response tests were performed using saline as diluent. However, saline was shown in this study to have an aggregating effect on the nanoparticles and the saline was exchanged for Milli-Q water. Serial 1:2 dilutions of the nanoparticles were done in a 96 well Nunclon plate. Milli-Q water was used as a control. AuNP were added to wells to final concentrations ranging between 8.1-260 µM Au. P-SPIO concentrations ranged between 3.1-100 µg/ml iron oxide. Final IXG-P concentration ranged between 0.87-28 mM Si. The final concentrations of S-SPIO were between 0.2–200 µg/ml iron oxide. All nanoparticle concentrations were added to triplicate wells. The cells were exposed to the nanoparticles for 24 h. When using CellTiter 96 AqueousOne Solution, 20 µl of the nanoparticle dilutions was added to 180 µl cell suspension in the 96 well plates. When using the CellTiter Blue, 10 µl of the nanoparticle dilutions series was added to 90 µl cell suspension.

Determining dose-resoponse

After 24 h exposure to nanoparticles the dose-response was determined. A working stock of CellTiter 96 AqueousOne Solution Cell Proliferation Assay reagent was prepared by mixing 2 ml AqueousOne reagent with 10 ml pre heated Phenol red free RPMI 1640 (supplemented as described above). Phenol red was excluded as phenol red absorbs at the same wavelength as formazan (490 nm). The cell culture medium was aspirated from all wells in the 96-well plate. Each well was washed with 100 µl PBS which was then aspirated. One hundred µl of assay working stock was added to each well. The plate was incubated for 2-4 hours. An absorbance micro plate reader (Spectra Max 340 PC from Molecular Devices) was used to measure absorbance at 490 nm and 650 nm. One hundred µl working stock assay regent was used as a blank.

When using CellTiter Blue, 20 µl of the regent was added per well without prior washing. The plates were incubated between 2-4 hours. The resazurin dye (blue) and the resorufin product (pink) are light-sensitive and prolonged exposure to light can result in increased background fluorescence and decreased sensitivity. Therefore the plates were covered in aluminium foil after reagent was added. The fluorescence signal was measured at $560_{Ex}/590_{Em}$ nm with a Polar Star Optima plate reader from BMG Labtech. Twenty µl CellTiter Blue reagent mixed with 100 µl cell culture medium was used as blank.

Nanoparticle interference with the fluorescence signal was tested when using the CellTiter Blue kit. 10 µl P-SPIO particles with a concentration of 1 mg/ml and 10 µl AuNP with a concentration of 2.6 mM was added to 10 wells 10 min prior to measurements. The procedure also allowed for investigation if nanoparticle toxicity occurred instantly.

2.5. Cellular uptake of nanoparticles

The concentrations of nanoparticles added to the cells were based on the results of the dose-response tests and previous publications [2, 35, 39]. Cells were seeded in 24 well or 6 well plates at different cell densities but in 0.9 and 3.6 ml cell suspension respectively. Cells were incubated overnight whereafter 100 µl (24 well plates) or 400 µl (6 well plate) nanoparticle solution was added per well on the plates. Water was used as control. The plates were incubated at 37°C for 4 or 24 h based on previous publications [2]. After exposure to nanoparticles, the cells were washed 3 times with pre-heated PBS. One hundred µl (24 well plates) or 400 µl (6 well plates) trypsin was added to the wells. The plates were incubated at 37˚C for 5 minutes. One point five ml (24 well plates) or 6 ml (6 well plates) cell culture medium was added to all wells to neutralize the trypsin. The solutions were transferred to sterile Eppendorf tubes. The tubes were centrifuged for 5 minutes at 4500×g and the supernatant was discharged. The cell pellets were washed with 500 µl (24 well plate) or 2 ml (6 well plate) PBS and centrifuged 5 minutes at 4500×g. The cell pellets were resuspended in PBS and the cell density was determined using a Bürker counting chamber. The cell suspensions were further analysed for element concentrations and/or relaxivity.

2.6. Prussian blue staining

Visual confirmation of iron uptake was done using a Prussian blue staining kit (Sigma Aldrich). Prussian blue is a histopathology stain for detecting the presence of iron. Stained iron is visualized as blue or purple deposits [2, 40].

A 96 well plate was seeded with 5000 HepG2 cells per well. Cells were incubated with 2, 20 and 50 µg/ml P-SPIO for 24 h. After incubation the cells were washed three times with PBS for removal of free P-SPIO particles. Cells were fixed with 4% paraformaldehyde for 40 min and thereafter washed three times with PBS. The cells were incubated for 10 min with Pearls reagent (4% potassium ferrocyanide and 12% HCl 1:1). The wells were washed three times with PBS and stained for one minute with neutral red and observed in a microscope.

3. Results and Discussion

3.1 Nanoparticle stability

The stability of nanoparticles can be altered depending on which solution they are diluted in. Instability can lead to aggregation which results in altered particle behaviour.

A-SPIO stability

Sedimentation was seen with A-SPIO in H_2O, saline and cell culture medium with and without FBS indicating that these particles were very unstable. Relaxivity was measured on filtered and non-filtered PEGylated A-SPIO for comparison of iron content. A smaller amount of iron was seen in the filtered sample. Sonication (50 x 5 sec) was done on both solutions whereafter the solutions were viewed in a microscope. Aggregates were seen in both solutions. An increase in both T_1 and T_2 was seen over a time period of 15 minutes with three relaxivity measurement on the same sample. This indicated decreasing concentrations of iron in samples with time which was confirmed by visual confirmation of a brown layer at the bottom of the sample tubes. The results indicated that PEGylated A-SPIO and the un-PEGylated A-SPIO were not stable and were therefore not further used.

Naked SPIO stability

Sedimentation of naked SPIO nanoparticles was seen in samples with saline and cell culture medium with and without FBS. However no sedimentation was seen in H_2O. Sedimentation of SPIO nanoparticles coated with PEG500 and polyacrylic acid was seen in all solutions. This indicated that the naked SPIO, SPIO coated with polyacrylic acid and PEG500 were unstable.

P-SPIO, S-SPIO, AuNP and IXG-P stability

P-SPIO, S-SPIO, AuNP and IXG-P nanoparticles were stable in saline, H_2O and cell culture medium with and without FBS as no sedimentations were seen.

3.2. Size and concentration of nanoparticles

The concentration of iron, gold and silicon in filtered stock solutions were determined by ICP.

Naked SPIO nanoparticle coated with PEG1000 (P-SPIO)

The iron concentration in filtered working stock (diluted 1:70 from 7 % original stock solution) P-SPIO was 53.6 mM. According to the product specification the iron concentration in a corresponding dilution was 64.8 mM in the non-filtered SPIO. Thus a small amount of iron was lost in filtration.

The size distribution of naked SPIO in H_2O as determined by DLS ranged between 50 nm to 700 nm which indicated possible aggregation. The size of P-SPIO in H_2O was in average 72 nm. When the PEG molecules were added the aggregations might have been dissolved, separating the P-SPIO aggregates into individual particles. The size of P-SPIO in saline was larger (1184 nm) compared to in water. This indicated that the particles tend to form aggregates in saline though no visual confirmation of aggregates formation in saline was seen. Thus, dilutions were hereafter done with water. The size of the particles in cell culture medium with and without FBS indicated larger size of the particles (>100 nm) compared to the measurement in water. This phenomenon was most likely due to increased viscosity. Cell culture medium is more viscous than water and the particles therefore move slower with the effect of particles appearing larger than their actual size. To obtain the accurate size of the nanoparticle they were preferably measured in water.

H-SPIO measured in water had an average size of 105 nm. This might be due to larger amounts of PEG molecules attached onto the surface of the SPIO enlarging the molecule.

SPIO nanoparticle coated with APTMS (S-SPIO)

The presence of APTMS coated onto the SPIO was examined by ninhydrin staining. The filter paper was coloured purple, which indicated that SPIO was successfully coated with APTMS. The iron concentration of S-SPIO was determined by ICP to be 22mg/ml. The size of the filtered particles was determined with DLS to be 68-78 nm.

Gold nanoparticles

Gold is a very unreactive metal and requires strong acid such as aqua regia to break its bonds and bring it into solution. ICP analysis of the AuNP indicated that the gold concentration of the stock solution was 26.91 mM. Size determination by DLS indicated that the AuNP were 10-11 nm. The coating percentage was previously calculated to be 32% meaning that the outer surface of the particle is coated with 32% sulphur [41]. As each PEG was attached to two sulphurs the percentage of gold that is coated with PEG was 16%.

Determination of particle loss during filtration was done by measuring an absorbance spectrum of a sterile filtered and non-filtered AuNP solution diluted to 130 µM in water. The resulting spectrum is seen in Figure 3.

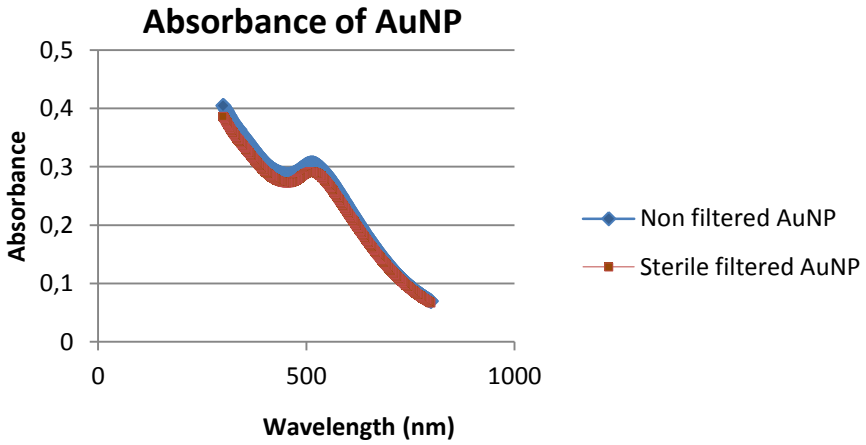

Figure 3. Absorbance was measured on sterile filtered gold nanoparticles solution and non-filtered nanoparticles solution to investigate if particles were lost during filtration.

Both solutions had an absorbance peak at 513 nm. The filtered AuNP had a nearly identical spectrum compared to the non-filtered AuNP which indicates that hardly any particles were lost during filtration. The small difference might be due to precision in dilution.

Ion-X-gel precursor (IXG-P)

The ICP analysis indicated that the silicon concentration in IXG-P was 45.5 mM. The concentration was too low for downstream experiments and the particles were concentrated by spin filtration with Amicon Ultra 10 kD filters (Millipore) at 4000×g for 30 min. After the spin filtration, the silicon concentration was determined to 343 mM with ICP analysis. Size determination of the particles by DLS was not possible in water due to similar refraction index of the particles and water. Saline, however, has a different refraction index compared to the particles and the size could be determined to 4-5 nm. The size had previous been confirmed by co-workers at Spago Imaging AB using high-performance liquid chromatography (HPLC).

3.3. Dose-response assessment

In order to establish if the nanoparticles used in this work have toxic effect on cells, dose response tests were performed. HepG2 and MDA-MB-231 cells were incubated with different concentrations of P-SPIO, H-SPIO, S-SPIO, AuNP and IXG-P nanoparticles.

In dose-response tests using Aqueous One, a dip in cell number was seen in the most outer wells of the plates (see Figure 4). This was thought to be due to insufficient mixing of the seeding cell culture resulting in an uneven distribution of cells in the suspension. HepG2 cells have a tendency to aggregate and this could also create an uneven number of cells in the wells. In the repeated dose-response tests the cell cultures were pipetted repeatedly with a 1 ml pipette and the cell suspension was vortexed before being added to the 96 well plates in order to obtain an even distribution of cells in all wells. The cells

were also added to the wells in a random order and the nanoparticles were not added in the outer most wells. The dip was still seen but to a smaller degree.

Comparison of CellTiter Blue and AqueousOne dose-response tests

Dose-response tests with HepG2 cells incubated with IXG-P nanoparticles were done simultaneously using the two different test kits. Comparison of CellTiter Blue test and AqueousOne indicated that more accurate measurements were obtained with CellTiter Blue. Smaller standard deviations were seen with CellTiter Blue and the uneven values seen at the lowest concentrations of nanoparticles observed when using AqueousOne were not seen with CellTiter Blue. The same results were seen with all cell types both with and without nanoparticles. The overall dose-response appeared to be lower when using AqueousOne test. Stabilization was seen at 80 % with AqueousOne while stabilization at 100% dose-response was seen with the same concentration of nanoparticles using CellTiter Blue. The reason for this was unclear. Thus, CellTiter Blue kit was used for dose-response testing. A comparison of CellTiter blue test and AqueousOne is seen in Figure 4.

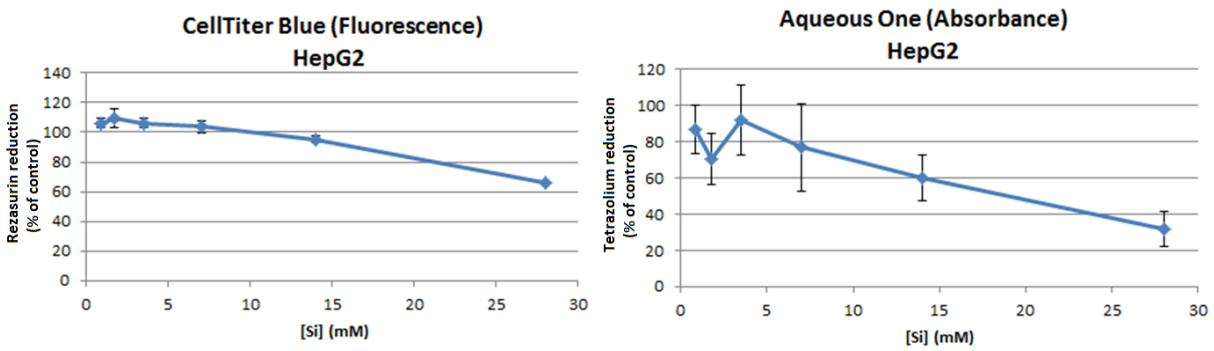

Figure 4. Comparison of AqueousOne and CellTiter Blue dose-response kits on HepG2 cells incubated with IXG-P nanoparticles.

Nanoparticle interference with the fluorescence signal was tested when using the CellTiter Blue kit. The results indicated that the fluorescence signal was not affected by the addition of P-SPIO particles and AuNP 10 min prior to measurements (results not shown).

MDA-MB-231 and HepG2 cells incubated with AuNP, P-SPIO and IXG-P

Results from dose-response tests using CellTiter Blue kit with MDA-MB-231 and HepG2 cells incubated with IXG-P, AuNP and P-SPIO are presented in Figure 5. HepG2 cells were less sensitive to IXG-P particles compared to MDA-MB-231 cells. Both cell lines were resistant to the full range of concentration of AuNP.

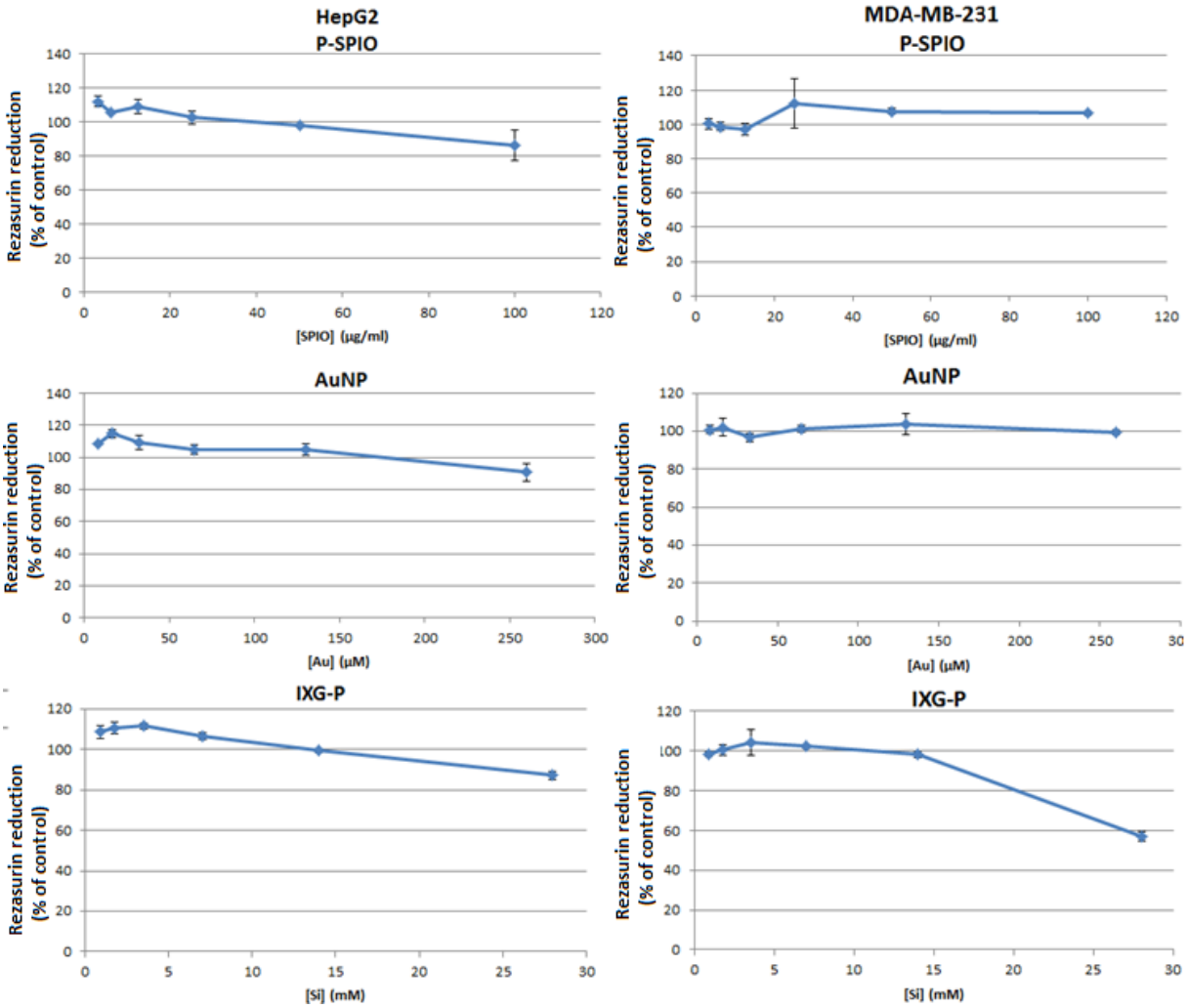

Figure 5. The dose-response of MDA-MB-231 and HepG2 cells incubated with P-SPIO, AuNP and IXG-P nanoparticles. Note the difference in Y-axis max.

MDA-MB-231 and HepG2 cells incubated with P-SPIO and H-SPIO

The dose-response of MDA-MB-231 and HepG2 cells were tested with H-SPIO using the AqueousOne kit. This dose-response tests was done before it was discovered that CellTiter Blue was a more accurate method. The results are presented in Figure 6. The HepG2 cells indicated no difference in cell number between the cells incubated with H-SPIO and the cells incubated with P-SPIO. The MDA-MB-231cells were more sensitive to the H-SPIO compared to the P-SPIO. This might be due to difference in concentration of PEG molecules coated onto the surface due to elevated temperature when PEGylation of the particles was performed which might have led to a larger internalization of iron which could have toxic effects on the cells.

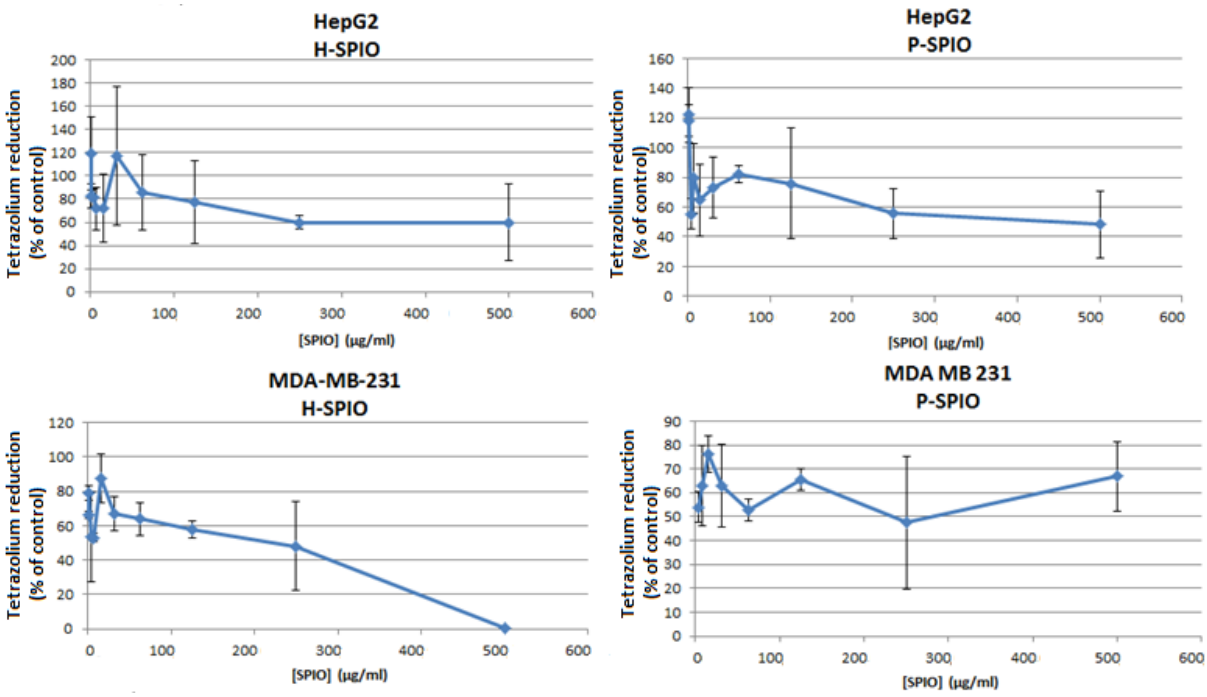

Figure 6. The dose-response of HepG2 and MDA-MB-231 cells incubated with P-SPIO and H-SPIO for 24 h. Note the difference in Y-axis maximum.

HepG2 cells incubated with S-SPIO

Dose-response tests with HepG2 cells incubated with S-SPIO particles are presented in Figure 7. The HepG2 cells were unaffected by all concentrations of S-SPIO.

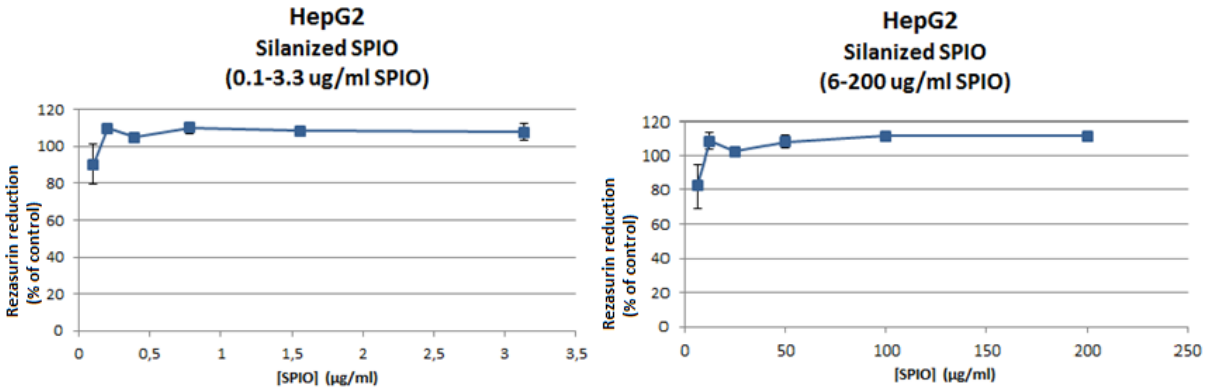

Figure 7. The dose-response of HepG2 cells incubated with S- SPIO nanoparticles.

3.4. Cellular uptake of nanoparticles

The aim of this part of the study was to find the optimal conditions for nanoparticle uptake with regards to cell density, cell culture area, nanoparticle concentration and harvest technique. Cells were cultured in 24 well plates or 6 well plates with different cell density. Cells were incubated with different concentrations of nanoparticles with different exposure times and the concentrations of internalized nanoparticles were determined. The hypothesis was that the degree of uptake would increase with increasing concentrations of nanoparticles. The concentrations of the nanoparticles

chosen in the uptake study were based on the results from the dose-response tests from section 3.3. and on previous publications [2, 35, 39].

Background control

The iron contents in the cells were in the first uptake experiments determined by the thiocyanate- and ferrozine methods which are both based on the measurement of absorbance. First, it was investigated if debris from lysed cells could interfere with the absorbance measurements. MDA-MB-231 cells were harvested and prepared at a cell density of 10^6 cells/sample. Samples 1 and 2 were left untreated. P-SPIO was added in samples 3 and 4 in a known concentration. The samples were treated with 1:1 volumes of 4 M HCl and the solutions were heated for 24 h at 60°C. The following treatments were done; samples 1 and 3 were vortex whereafter an absorbance spectrum was measured both before and after centrifugation for 10 min at 12000×g. Thereafter both samples were mixed with 1M KSCN (volume ratio 1:1) and 1M H_2SO_4 (volume ratio 1:100) and absorbance spectrum were measured for each samples again. Samples 2 and 4 were mixed with 1M KSCN (volume ratio 1:1) and 1M H_2SO_4 (volume ratio 1:100) and absorbance spectrum were measured. Thereafter both samples were centrifuged for 10 min at 12000×g and absorbance spectrum was measured for each sample again. The results are presented in Figure 8.

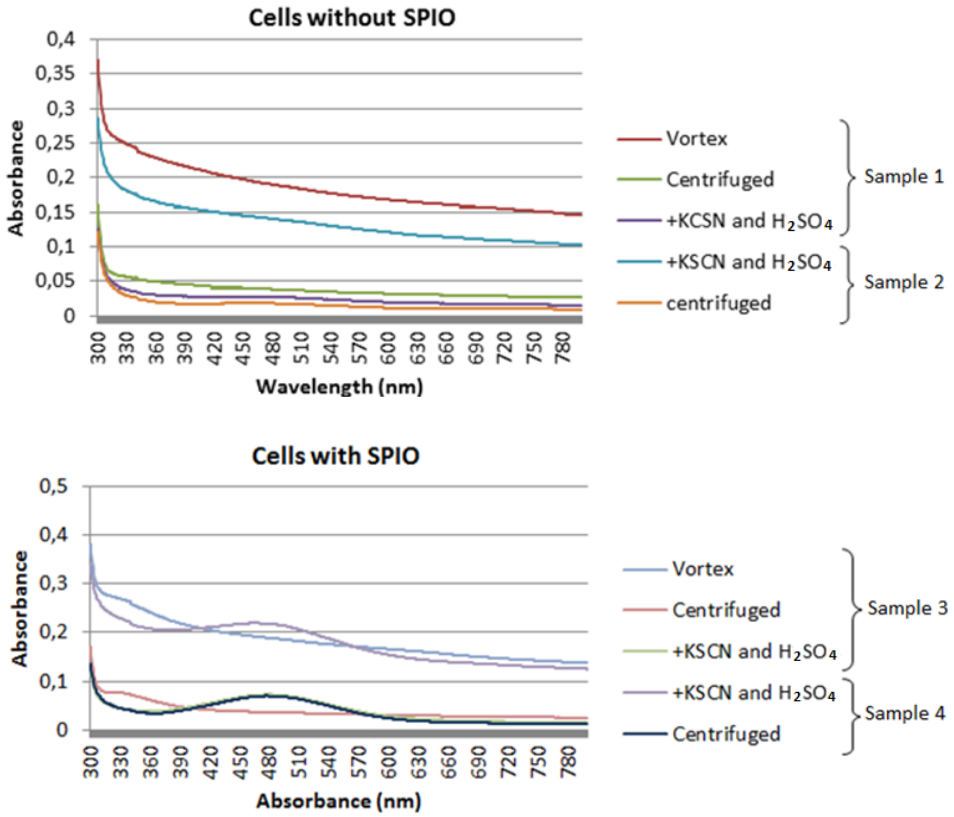

Figure 8. Sample 1 and 2 did not contain P-SPIO. Sample 3 and 4 contained P-SPIO. Sample 1 and 3 were vortexed, centrifuged and mixed with 1M KSCN and 1M H_2SO_4. Sample 2 and 4 were mixed with 1M KSCN and 1M H_2SO_4 and centrifuged. Absorbance was measured after each treatment.

A difference in absorbance was seen between non-centrifuged and centrifuged samples 1 and 2 indicating that rests from lysed cells could disturb measurements. Very little difference was seen between the two samples that were treated with KSCN and H_2SO_4 after centrifugation.

After incubation with KSCN and H_2SO_4, samples 3 and 4 both had an absorbance peak at 480 nm indicating the presence of iron, but differences in absorbance were seen between non-centrifuged and centrifuged samples 3 and 4. This indicated that rests from lysed cells could disturb measurements and therefore cell suspensions were centrifuged prior to measurements.

Development of nanoparticle uptake method

After examining the toxicity of the nanoparticles on the cells, a method for studying nanoparticles uptake in cells was developed by finding optimal method parameters. Two setups using AuNPs are presented below, whereupon six setups using P-SPIO are presented.

Influence of nanoparticle concentration and cell density on cellular uptake of AuNPs

Setup A

HepG2 cells were seeded in 24 well plates with a cell density of $1 \cdot 10^5$ and $7.4 \cdot 10^5$ cells/well respectively. AuNPs were added to the cells to the final concentrations of 0.4, 2, 10, 52, and 260 µM. The chosen gold concentrations were based on the results from previous publications [3, 17]. After incubation for 24 h the medium was discarded from the plates. For cell dissociation, trypsin/EDTA solution from Invitrogen formulated with 0.025% trypsin and 0.01% EDTA in PBS and trypsin neutralizer consisting of calf serum as a trypsin inhibitor was used as this was considered a mild treatment. The recommended incubation time with trypsin/EDTA solution was 1-3 minutes. After 3 minutes a large concentration of cells were still attached to the bottom of the wells and therefore the procedure with trypsin/EDTA and trypsin neutralizer was not used in further experiments. The cells were instead harvested using trypsin as described above. For determination of the Au concentrations, the samples were analysed with ICP. The results are presented in Figure 9.

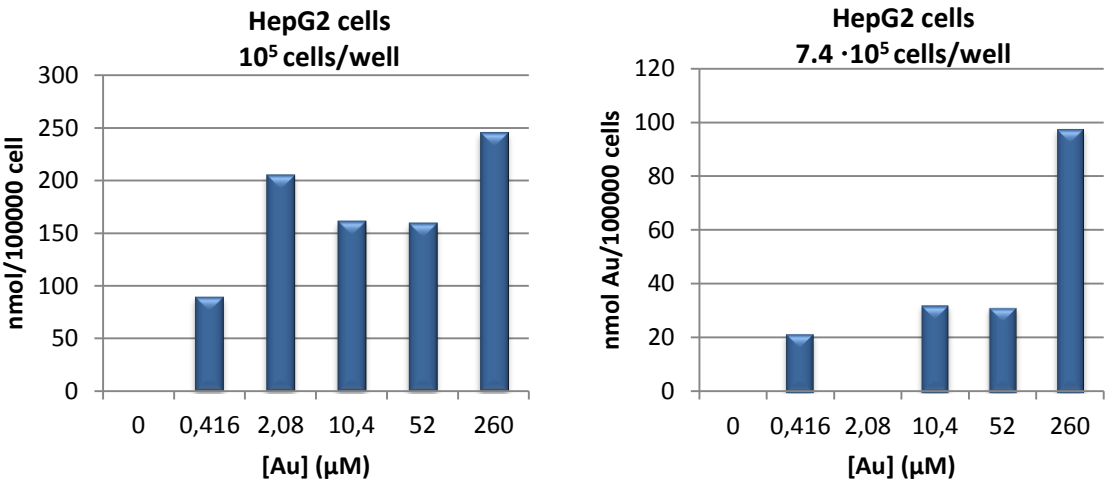

Figure 9. Intracellular Au content in HepG2 cells at 10^5 and $7.4 \cdot 10^5$ cells/well after 24 h incubation with gold nanoparticles with concentrations at 0.426-260 µM.

The desired result was an increase in uptake with increasing concentrations of AuNPs. The results indicated such a trend. The control wells at both cell densities contained no Au and a higher Au concentration was found in wells incubated with the highest concentrations of AuNP.

The results indicated that the seeded cell density of 10^5 was too low as the amount of gold was close to the ICP detection limit. In the wells with seeded cell density of $7.4 \cdot 10^5$ cells/well the cells were 100% confluent which indicated that this cell density was too high. In the following experiment the cell density was adjusted to $5 \cdot 10^5$ cells/well and three samples incubated with the same concentrations of AuNPs were pooled.

Setup B

HepG2 cells were cultured at a cell density of $5 \cdot 10^5$ cells/well in a 24 well plate. AuNPs were added to cell cultures to the final concentrations of 100, 20, 2 µM in nine wells per concentration. After incubation overnight, three wells per concentration were pooled prior to determination of the gold content in order to increase the gold concentrations in the samples. In addition, since each concentration was done in triplicate, standard deviations could be calculated. For determination of the Au concentrations, the samples were analysed with ICP. The results are presented in Figure 10.

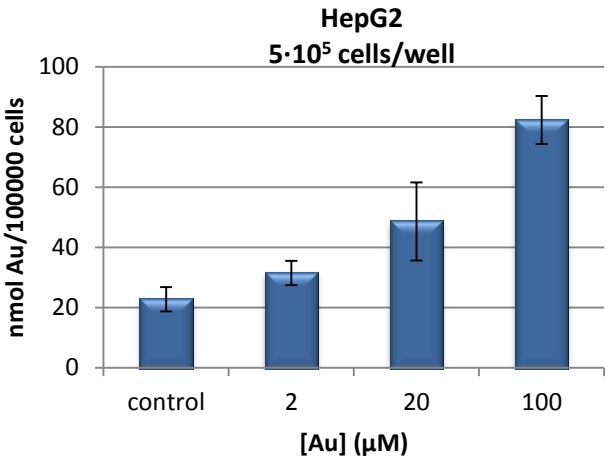

Figure 10. Intracellular Au content in HepG2 cells with $5 \cdot 10^5$ cells/well after 24 h incubation with gold nanoparticles with concentrations at 2-100 µM.

It was indicated that the cells were able to take up AuNPs of a size of 10 nm in a concentration dependent manner.

During uptake experiments with AuNPs, publications were found that included PEGylated gold nanoparticles as negative controls for cellular uptake, as it has been demonstrated that these do not bind to a variety of cancer cell lines in the absence of a specific targeting ligand [23]. Other publications have indicated that PEGylated AuNPs were taken up to a very low extent compared to other types of coatings [3]. Studies have also shown that uptake of AuNPs changed cellular morphology, increasing cell size and inducing apoptosis in cells [42]. The choice of using AuNP as a positive control in future experiments with other cell types can therefore be questioned. The AuNPs were not used in further experiments.

Influence of nanoparticle concentration, cell density and incubation time on cellular uptake of iron oxide nanoparticles

Setup A

The following parameters were used; HepG2 cells in a 24 well plate with seeding cell densities of $5 \cdot 10^3$, $1 \cdot 10^4$ and $1 \cdot 10^5$ cells/well. Incubation was done with P-SPIO nanoparticles with the final concentrations of 100, 50, 10, 4, and 2 µg/ml. After harvesting the cells, the cell pellets were resuspended in DMEM cell culture medium. The iron concentrations were determined with the thiocyanate method.

Iron was detected in the control samples indicating that there was a presence of iron in the medium. According to the manufacturer, DMEM contained 100 µg/ml $Fe(NO_3)_3$. In the following experiments the DMEM was replaced with PBS for resuspension of the cell pellets.

Other things were also observed. The cells were larger in the wells with the cell density 10^5 cells/well compared to the cells seeded at 10^4 and $5 \cdot 10^3$ cells/well. The reason for

this was unknown. More cell aggregates were observed in wells with seeded cell densities 10^4 and 10^5 cells/well compared to $5 \cdot 10^3$ cells/well.

In the following experiment, the cell pellets were resuspended in PBS and the cell density was increased to $1 \cdot 10^5$ and $7.4 \cdot 10^5$ cells/well.

Setup B

The following parameters were used; HepG2 and MDA-MB-231 cells were seeded in 24 well plates with seeding cell density of $1 \cdot 10^5$ and $7.4 \cdot 10^5$ cells/well. P-SPIO was added to the cells to the final concentrations of 100, 50, 10, 4, and 2 µg/ml and the plates were incubated. After harvesting of cells, the cell pellets were resuspended in 200 µl PBS. The iron content was determined with the thiocyanate method. The results are presented in Figure 11.

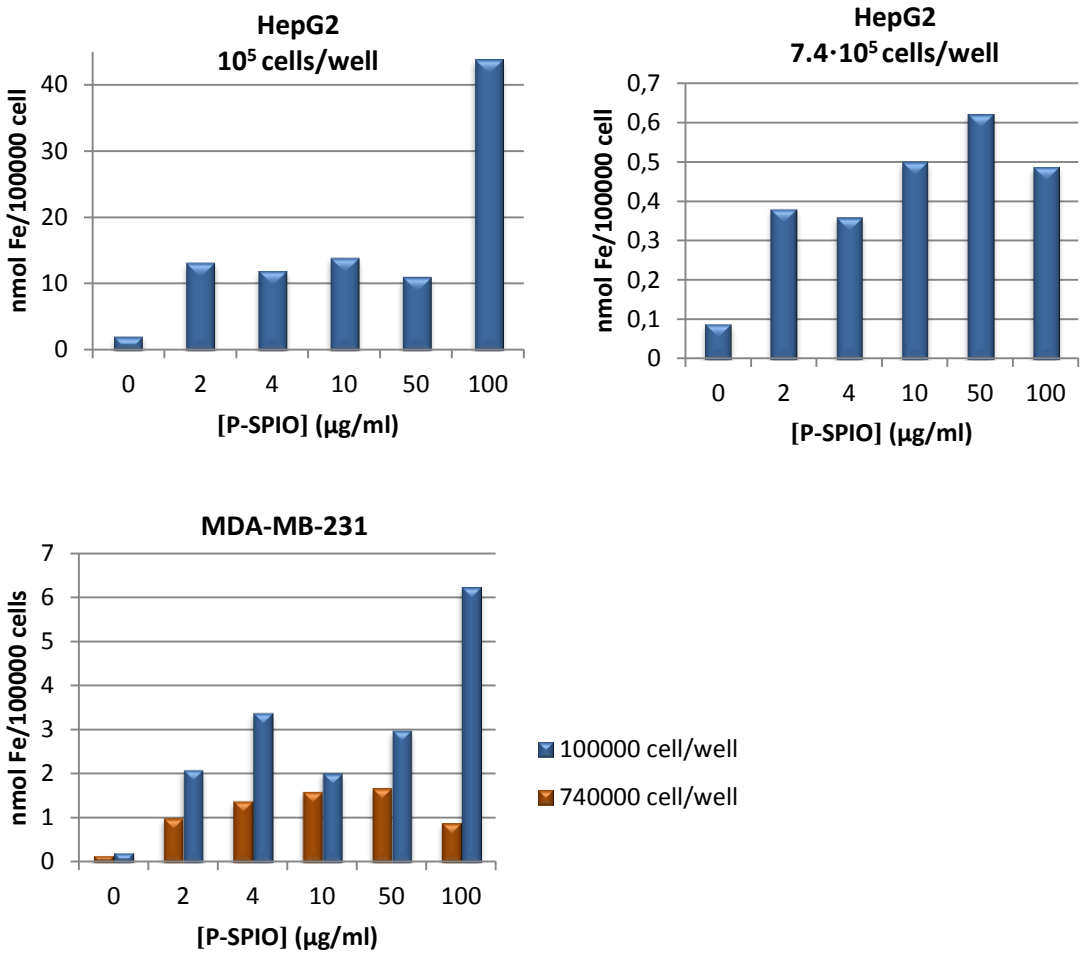

Figure 11. (Top left panel) Intracellular iron content in HepG2 cells with cell density at 10^5 cells/well after 24 h incubation with P-SPIO with concentrations ranging between 2-100 µg/ml. (Top right panel) Intracellular iron content in HepG2 cells with cell density at $7.6 \cdot 10^5$ cells/well after 24 h incubation with P-SPIO with concentrations ranging between 2-100 µg/ml. (Left bottom panel) Intracellular iron content in MDA-MB-231 cells with cell density of 10^5 and $7.4 \cdot 10^5$ cells/well after 24 h incubation with P-SPIO with concentrations ranging between 2-100 µg/ml.

Nanoparticle uptake with seeded cell density of $7.4 \cdot 10^5$ cells/well with both HepG2 and MDA-MB-231 cells indicated a tendency of concentration dependent uptake of P-SPIO. A higher uptake of iron was seen with higher concentrations of P-SPIO. In the wells with HepG2 cells seeded at 10^5 cells/well, the amount of cells after incubation with the highest concentration of P-SPIO, was 30% of the average amount of cells in the other wells. With MDA-MB-231 cells seeded at of 10^5 cells/well, the amount of cells after incubation with the highest concentration of P-SPIO was 80% of the average amount of cells in the other wells with MDA-MB-231 cells. This could indicate toxicity and therefore the calculated value of iron per 10^5 cells was misleading since the amount of cells was lower in these wells compared to the other wells.

A comparison between the two cell types, seeded with 10^5 cells/well, indicated that MDA-MB-231 cells internalized iron in a lower degree compared to HepG2 cells which correlated to previous publications [2]. This was not seen in cultures with a cell density of $7.4 \cdot 10^5$ cells/well.

The hypothesis that the degree of uptake would increase with increasing concentrations of P-SPIO was not consistent with a cell density of 10^5 cells/well. The iron concentrations were close to the detection limit of the thiocyanate method and were therefore not reliable. This could be due to too low cell density in relation to the concentration of P-SPIO. P-SPIO might have a too high impact on the low number of cells. In the wells with the cell density of $7.4 \cdot 10^5$ cells/well, the monolayer was 100% confluent. However, the total number of cells per well was lower than expected and this might be due to lack of surface area for attachment in relationship to the amount of cells indicating that the cell density was too high. However, at this cell density a tendency to an increase of intracellular iron was seen with increasing concentrations of P-SPIO, except for the highest incubation concentration at 100 µg/ml.

The results indicated that the seeded cell density of 10^5 cells/well was too low as the amount of iron was again close to detection limit. In the wells with seeded cell density of $7.4 \cdot 10^5$ cells the monolayer was 100% confluent which indicated that this cell density was too high. In the following experiment (see below) the cell density was adjusted to $3 \cdot 10^5$ and $5 \cdot 10^5$ cells/well and the samples were done in triplicate and they were pooled in an attempt to find the optimal cell density for attachment of all cells and cell amount large enough for obtaining detectable levels of iron.

Setup C

MDA-MB-231 cells were seeded with cell densities of $3 \cdot 10^5$ and $5 \cdot 10^5$ cells/well. The cells were incubated for 4 h with P-SPIO at concentrations between 0.5-50 µg/ml. HepG2 cells were seeded with same cell density as MDA-MB-231 but they were exposed to the nanoparticles for 24 h. Due to a calculation error the P-SPIO concentration of 50 µg/ml was not included in the setup. The concentrations of P-SPIO were instead 0.5-5 µg/ml. Concentration determination was done with the thiocyanate method. The results are presented in Figure 12.

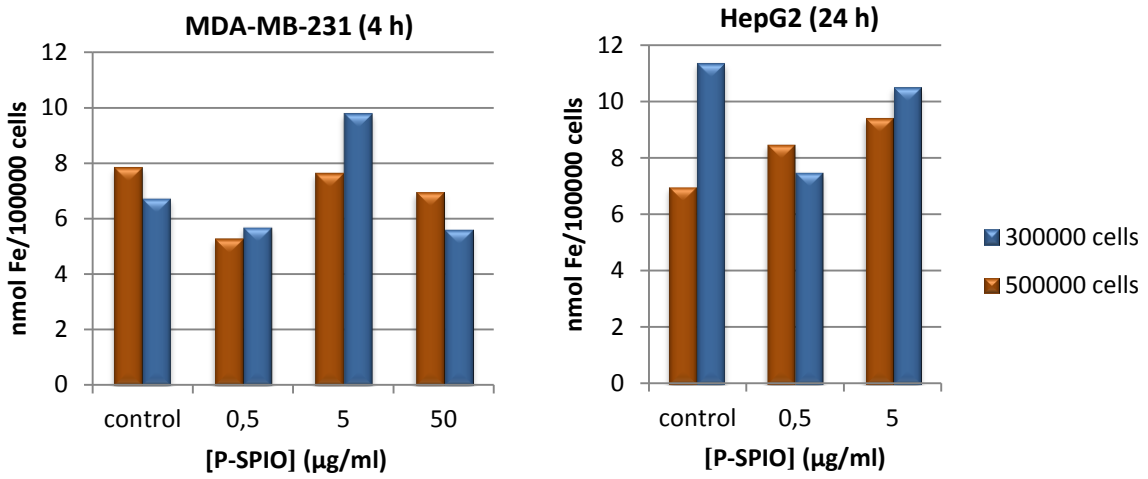

Figure 12. (Left panel) Intracellular iron content after 4 h incubation with SPIO concentrations at 0.5-50 µg/ml at 37°C in MDA-MB-231 cells with cell density of $3{\cdot}10^5$ and $5{\cdot}10^5$ cells/well (Right panel) Intracellular iron content after 24 h incubation with SPIO concentrations at 0.5-5 µg/ml at 37°C in HepG2 cells with cell density of $3{\cdot}10^5$ and $5{\cdot}10^5$ cells/well.

The amount of intracellular iron in all MDA-MB-231 cell samples was very low and did not correlate with the concentration of added P-SPIO. In addition, the amount of intracellular iron in the control cells was equal that of the cells incubated with P-SPIO. This might be due to an insufficient amount of cells used in the study since the resulting iron concentrations were very close to detection limit. The short exposure time could also contribute to the low concentrations, but since a longer exposure time using HepG2 cells gave similar results with the cell density $3{\cdot}10^5$ cells/well, the exposure time is most likely not the limiting factor. This was confirmed in pervious publication [39] which indicated that iron oxide complexes were attached to the surface rather than internalized after 4 h exposure. Thus, a nanoparticles exposure time of 4 h was not investigated any further. In the wells with HepG2 seeded at $5{\cdot}10^5$ cells/well, the uptake followed a concentration dependent trend. However, the background was still high in the control samples. In these wells the cell monolayer had not reached 100% confluency, indicating that enough surface was available for attachment for all the cells at this cell density.

Setup D

HepG2 cells were seeded in 24 well plates with a cell density of $3{\cdot}10^5$ cells/well. It was not possible to test a cell density of $5{\cdot}10^5$ cells/well as the amount of cells in the culture flasks were too low. P-SPIO was added to wells in triplicates at 0.5, 5 and 50 µg/ml whereafter the plates were incubated. Concentration determination after harvesting of the cells was done with the thiocyanate method. The results are presented in Figure 13. Despite the increased cell amount, the values were close to the detection limit and could therefore not be trusted. The result with the HepG2 cells were similar to the previous experiments (see above) in that the uptake of iron seemingly increased with increasing P-SPIO concentrations. Unfortunately, the iron concentration in the control cells was too high.

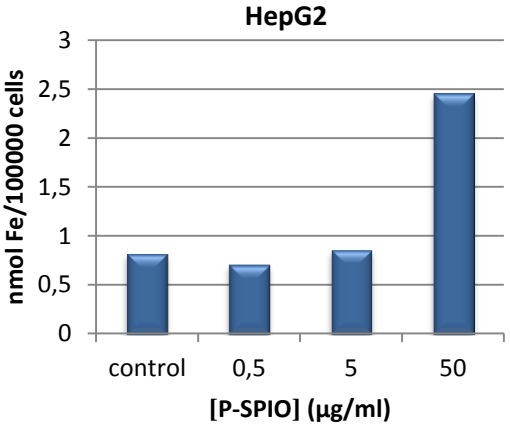

Figure 13. Intracellular iron content in HepG2 cells with cell density of $3 \cdot 10^5$ cells/well after 24 h incubation with P-SPIO with concentrations at 0.5-50 µg/ml.

Setup E

Simultaneously as the previous experiment with HepG2 cells was done (Attempt D) the same parameters were tested on MDA-MB-231 cells in 24 well plates but also including an experiment in 6 well plates. Cells were seeded at $3 \cdot 10^5$ and $5 \cdot 10^5$ cells/well in 24 well plates together with 6 well plates with $1 \cdot 10^6$ cells/well. P-SPIO was added to the wells with final concentrations from 0.5-50 µg/ml. Iron concentrations were determined with the thiocyanate method. The results are presented in Figure 14.

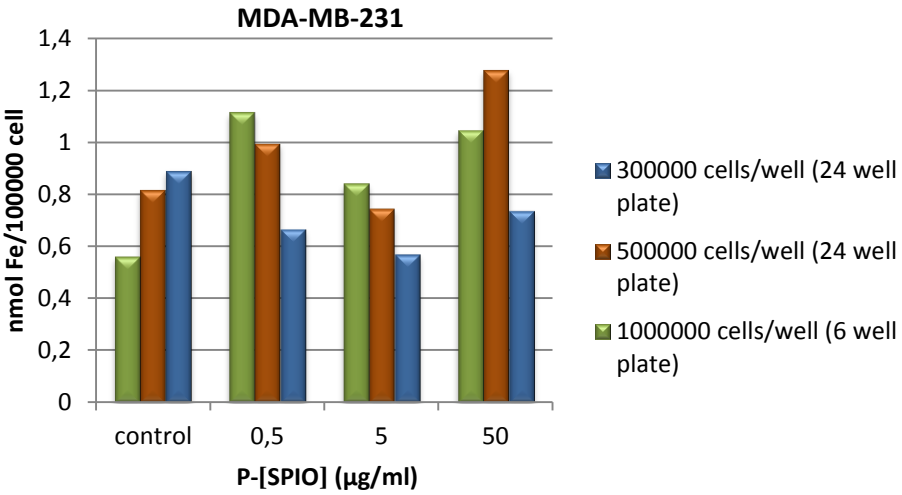

Figure 14. Intracellular iron content in MDA-MB-231 cells with cell density of $3 \cdot 10^5$ and $5 \cdot 10^5$ cells/well in a 24 well plate and 6 well plate with a cell density of $1 \cdot 10^6$ cells/well after 24 h incubation with P-SPIO with concentrations at 0.5-50 µg/ml.

The resulting iron concentrations were very close to the detection limit. The control samples for the cells seeded at $3 \cdot 10^5$ and $5 \cdot 10^5$ cells/well had high iron concentrations. It was assumed that the cell density was too low for obtaining detectable iron amounts.

The iron concentrations in the 6 well plates were not reliable as the concentrations were very close to the detection limit.

Comparison between the two cell type in 'Attempt D' and 'Attempt F' with cell density of $3 \cdot 10^5$ cells/well incubated with 50 µg/ml P-SPIO indicated that MDA-MB-231 cells internalized iron to a lower degree compared to HepG2 cells which correlated with previous publications [2].

In the following experiment (Attempt F) a cell density of $5 \cdot 10^5$ cells/well was used as the cells at this cell density had the ability of proliferating in a non-inhibiting way. Pooling of samples incubated with the same concentration of P-SPIO was done in order to obtain detectable amounts of iron.

Setup F

HepG2 cells were seeded in 24 well plates with a cell density of $5 \cdot 10^5$ cells/well. P-SPIO was added to wells in triplicates per iron concentration. After harvesting of cells, triplicates were pooled in order to increase the iron concentration. The iron concentration was determined with the ferrozine method. The amount of iron was below detectable levels and no results were obtained. In the following experiments the concentrations of iron were increased by pooling of five samples, and the samples were analysed with ICP.

The successful assay setup

HepG2 cells were seeded in 24 well plates with a cell density of $5 \cdot 10^5$ cells/well. P-SPIO was added to the final concentration of 50, 20 and 2 µg/ml in 15 wells per concentration. Following exposure and cell harvest, 5 samples per concentration were pooled giving triplicates for each concentration. The samples were analysed for T_1 and T_2 relaxivity and iron content. ICP analysis was more sensitive in determination of low iron concentrations and therefore this method was used instead of the thiocyanate and the ferrozine method. The results are presented in Figure 15. The iron concentrations were well above the ICP detection limit which indicated that the results were reliable.

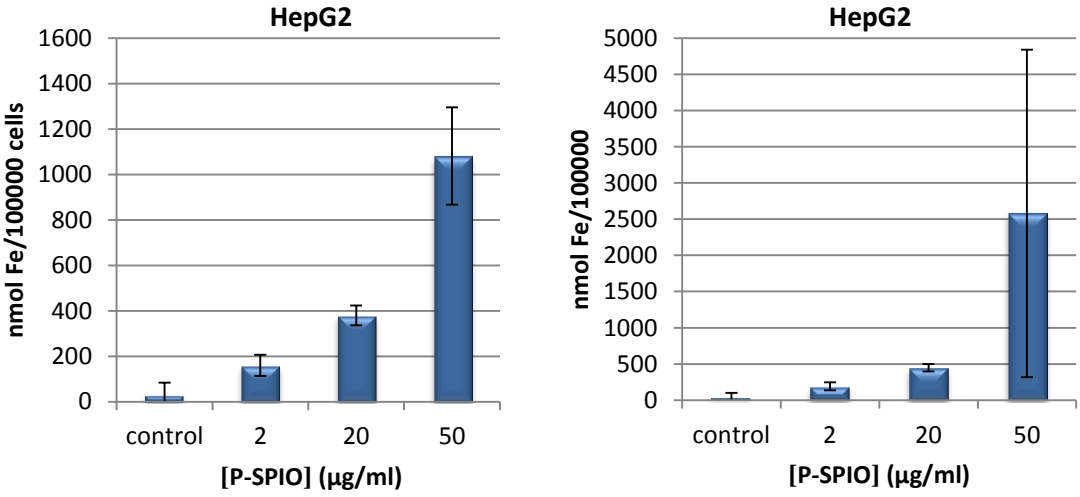

Figure 15. Intracellular iron content in HepG2 cells with cell density of $5 \cdot 10^5$ cells/well in a 24 well plate after 24 h incubation with P-SPIO with concentrations at 2-50 µg/ml at 37°C. In the left panel one of the triplicate samples at 50 µg/ml P-SPIO was excluded. See text for further discussion.

The results indicated a clear increase of uptake of iron in HepG2 cells with increasing incubation concentration of P-SPIO. The highest uptake was seen with the P-SPIO concentration of 50 µg/ml. No effect on cell number was seen at this concentration as the number of cells counted in these wells was equal to the number of cells counted in the control wells. One of the triplicates from the wells incubated with 50 µg/ml was excluded in the left panel in Figure 14 as this had a substantial higher iron content compared to the other two samples with the same incubation concentration. After communication with the staff at the ICP lab it was concluded that this could be due to iron contaminants from calibration samples in the machine at the ICP lab. On the right panel in Figure 14 the outlier at 50 µg/ml is included.

T_1 and T_2 relaxivity were also measured on cell samples prior to ICP analysis (see Figure 16). Both T_1 and T_2 increased with decreasing incubation concentrations of P-SPIO. This indicated that the intracellular iron content was increased with increasing incubation concentrations of P-SPIO.

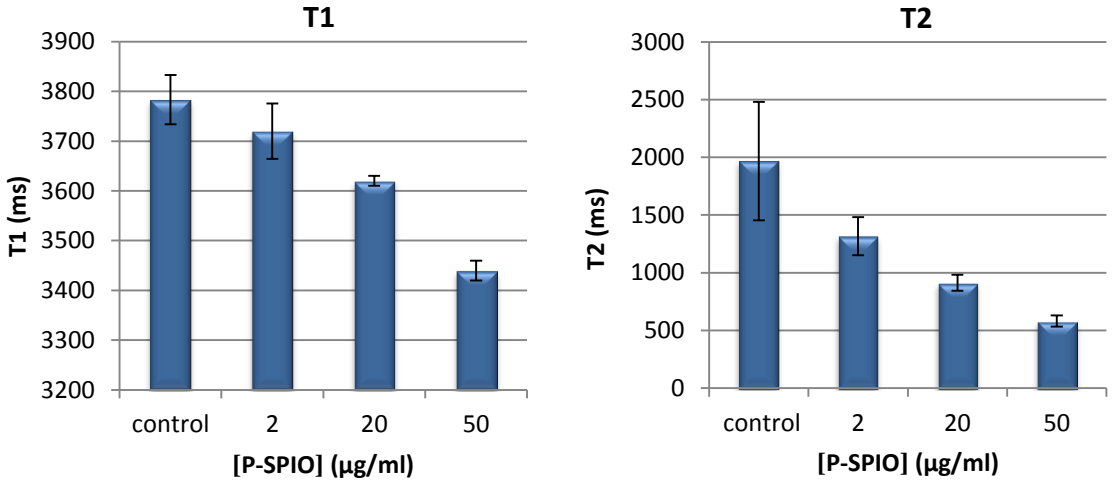

Figure 16. The T1 (left) and T2 (right) were measured on HepG2 cells incubated with concentrations of SPIO between 2-50µg/ml. Water was used as a control. A higher T value indicates a lower iron concentration in the sample.

The experiment described above was repeated with the same parameters to confirm the results. Iron concentrations were determined with ICP. Results are presented in Figure 17.

Particles can be attached to the outer membrane of the cells, without particle uptake. This may result in faulty iron values and to rule out particle contamination the following procedure was done; 10 minutes before the cells were harvested, P-SPIO was added to wells in the 24 well plates to a concentration 50 µg/ml. No iron was detected in the cells (see Figure 17).

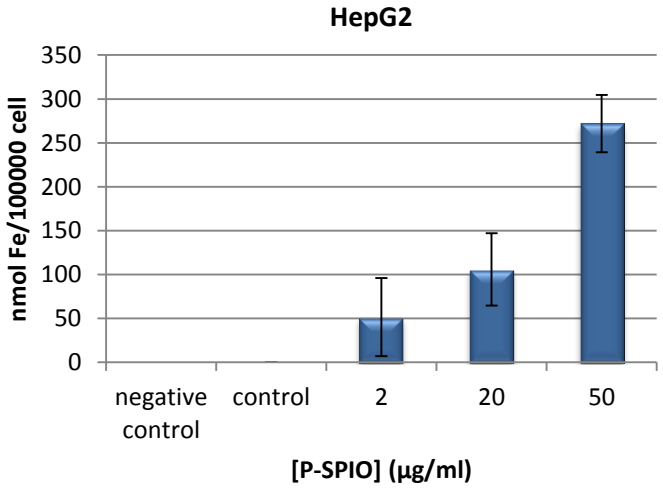

Figure 17. Intracellular iron content in HepG2 cells seeding at $5 \cdot 10^5$ cells/well after 24 h incubation with P-SPIO with concentrations at 2-50 µg/ml with water added as control. Contamination of cells with particles was investigated with addition of P-SPIO 10 minutes prior to cell harvesting (negative control).

The iron content in the cells was lower compared to the previous experiment (see Figure 16) but the trend was similar. The ICP laboratory suggested that an error could

have been made at the lab when diluting the samples prior to analysis. The standard deviation did overlap with the concentrations at 20 and 2 µg/ml but as the control did not contain any iron the results were considered reliable. The potential dilution error at the ICP lab was strengthened with the results from the T_1 and T_2 measurments (see Figure 18) which resulted in similar relaxation values as the previous experiment. Internalization of iron was seen in a concentration dependent manner.

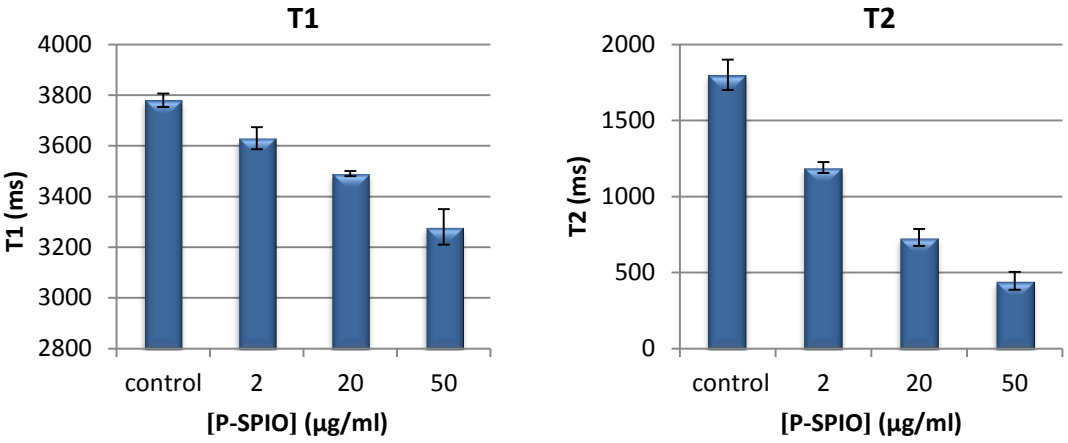

Figure 18. The T1 (left) and T2 (right) were measured on HepG2 cells incubated with concentrations of SPIO between 2-50 µg/ml. Water was used as a control.

The values of T_1 and T_2 in the samples tested with P-SPIO particles added just prior to the harvesting of cells were similar to the water control indicating that no iron contamination occurred (results not shown).

The experiments resulted in detectable internalization of P-SPIO in HepG2 cells, indicating that the P-SPIO particles could be used as positive control in further experiments. The amount of iron content in the cells incubated with P-SPIO at 50 µg/ml correlates well to previous publications [39, 43, 44]. P-SPIO nanoparticles at an incubation concentration of 50 µg/ml were used as a positive control in following experiments using the same set up but with other nanoparticles.

Prussian Blue staining

Prussian Blue staining was done to visually confirm the intercellular location of internalized iron. Accumulation of iron was seen as black spots (see Figure 19) in the cytoplasm of HepG2 cell incubated with 50 µg/ml P-SPIO. In which organelle the accumulation occurred was not determined. These accumulations were not seen in the cells incubated with lower concentrations of P-SPIO or in the control cells. This was an indication of the ability of HepG2 cells to take up P-SPIO and it supports the results in the adsorption test, i.e. that nanoparticles are not adsorbed to the surface of the cells.

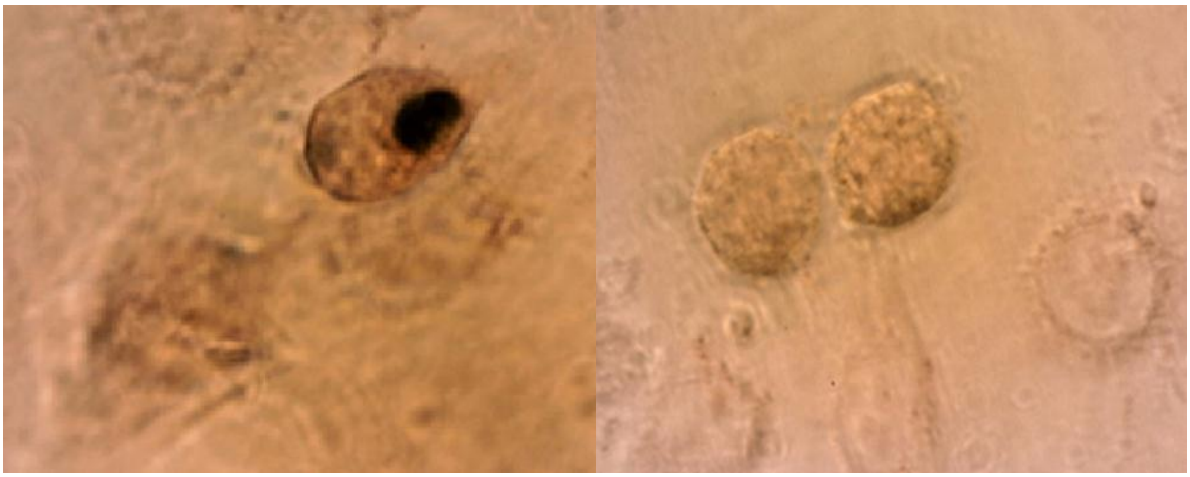

Figure 19. Accumulation of iron is seen as a black spot in the cytoplasm of the HepG2 cell (left). No accumulation of iron was seen in control cells without any SPIO (right).

Uptake of S-SPIO

To compare how different coatings affect the degree of uptake, HepG2 cells were exposed to S-SPIO and P-SPIO. Six well plates with HepG2 cells were prepared with a seeded cell density of $2.5 \cdot 10^6$ cells/well. P-SPIO and S-SPIO were added to wells in triplicates to the final concentrations of 50 µg/ml. Cells were harvested after 24 h and the pellets were resuspended in PBS and the cells were counted. ICP analysis was not performed on the samples. Instead T_1 and T_2 were measured on the cell suspensions (see Figure 20). The results indicated higher iron content in cells incubated with S-SPIO compared to cells incubated with P-SPIO.

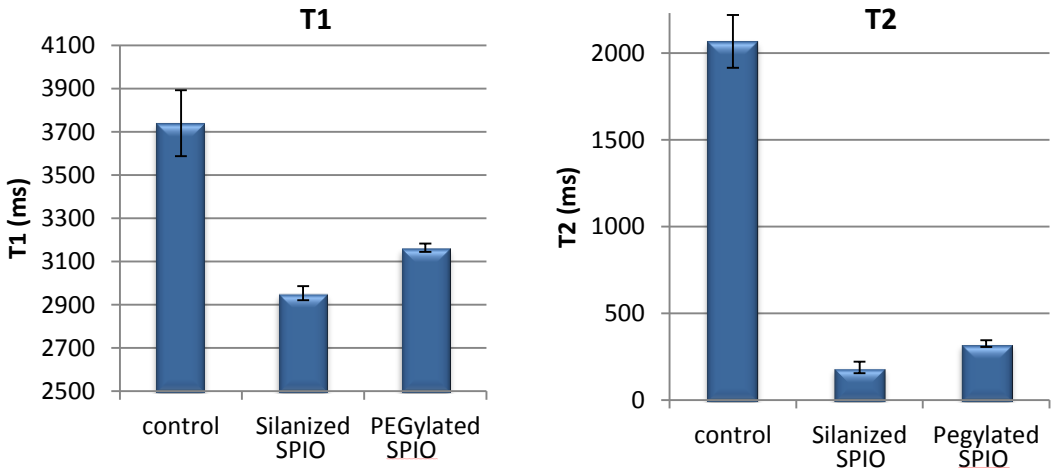

Figure 20. The T1 (left) and T2 (right) were measured on HepG2 cells incubated with silanized and P-SPIO at 50 µg/ml. Water was used as a control.

Uptake of IXG-P

When the method for studying cellular uptake was established it was used to investigate if HepG2 cells had the ability of internalize Spago Imagings Ion-X-Gel precursor. HepG2 cells were cultured at a cell density of $5 \cdot 10^5$ cells/well in a 24 well plate. IXG-P particles were added to 15 wells per concentration to the final concentration of 15, 7.5 and 2 mM silicon. Fifty µg/ml P-SPIO was used as reference. Following exposure and cell harvest, 5 samples were pooled giving triplicates of each concentration. The silicon and iron content was determined by ICP analysis. Results are presented in Figure 21.

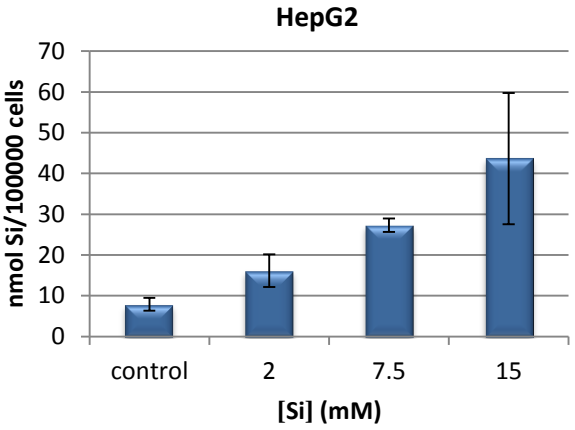

Figure 21. Intracellular silicon content in HepG2 cells after 24 h incubation with different concentrations of IXG-P nanoparticles. P-SPIO nanoparticles with a concentration of 50 µg/ml were used as reference particles (results not shown).

The uptake of IXG-P occurred in a concentration dependent manner. As incubation concentrations with IXG-P particles increased the concentration of internalized nanoparticles increased. The iron content in the cells incubated with P-SPIO was measured. The iron content was in the same range as in previous trials, 1.1 µmol/10^5 cells (see 'successful assay setup') confirming the function of the set up and the cells ability to internalize nanoparticles. This indicated that HepG2 cells had the ability to internalize IXG-P nanoparticles.

4. Conclusions

In the presented thesis an *in vitro* based assay was developed for studying cellular uptake of nanoparticles. The assay was used to analyse the interaction between IXG-P and HepG2 cells with respect to cellular uptake. Reference nanoparticles to be used as positive controls needed to be included in the experiments in order to confirm the function of the set up. Three different reference nanoparticles were investigated. Superparamagnetic iron oxide nanoparticles (SPIO), which were modified with PEG and APTMS, and PEGylated gold nanoparticles. The dose-response of HepG2 and MDA-MB-231 cells incubated with the three different nanoparticles including IXG-P was tested. The dose-response tests indicated at which nanoparticles concentrations the particles were toxic to the cells. Two dose-response kits were used, CellTiter Blue and AqueousOne. The use of CellTiter Blue kit was preferred as this method gave lower standard deviations and it was more cost efficient compared to the AqueousOne kit. Method development for studying uptake of nanoparticles in HepG2 and MDA-MB-231 cells was based on the results of the dose-response tests and results from previous publications. Parameters such as cell density, nanoparticle concentration and exposure time to the nanoparticles were changed in different setups in order to ultimately achieve detectable and repeatable uptake of the nanoparticles in the cells.

The internalization of 70 nm PEGylated SPIO and 10 nm gold nanoparticles was seen in HepG2 cells in a dose dependent manner with the following parameters;

- 24 well plates with seeded cell density of $5 \cdot 10^5$ cells/well
- exposure time of nanoparticles for 24 h
- using trypsin for harvesting of the cells
- resuspension of the cell pellets in PBS
- pooling of 5 samples following harvesting of cells
- concentration determination using ICP-AES

The concentration of the internalized PEGylated SPIO was preferably determined with ICP-AES as this method was more sensitive with lower detection limit in comparison with the thiocyanate- and the ferrozine methods where the detection limits were too high. The major difficulty with ICP-AES is the associated higher cost. The uptake of PEGylated SPIO was also confirmed with relaxivity measurments, where the values of T_1 and T_2 increased with decreasing incubation concentrations of P-SPIO. This indicated that the iron contents in the cells increased with increasing incubation concentrations of P-SPIO. The highest uptake in HepG2 cells was seen with incubation concentration of 50 µg/ml P-SPIO. The intercellular location of iron was visually confirmed with Prussian Blue staining.

The results indicated that a successful method for studying uptake of nanoparticles using PEGylated SPIO at a concentration at 50 µg/ml as a positive control was achieved.

The internalization of the IXG-P with the size of 5 nm was tested in HepG2 cells using the PEGylated SPIO particles as a positive control. IXG-P was internalized in a dose dependent manner. A comparison of uptake between silanized and PEGylated SPIO was tested in HepG2 cells. The results indicated a higher uptake of the silanized SPIO particles compared to the PEGylated SPIO particles.

5. Proposed future work

The rate, mechanism and the degree of internalization of nanoparticles have been indicated to be very cell-type dependent and varies between nanoparticles depending on their size, charge, and other surface properties [25]. Publications have indicated that non coated SPIO particles are internalized by tumour cells at a lower degree compared to coated SPIO particles [31]. It has also been indicated that PEG coating can both facilitate the uptake of iron and decrease the uptake depending on the cell type. Different PEG molecules differ in size and the type of PEG chosen as coating molecule can result in difference in uptake. Therefore, different coatings of SPIO can be evaluated in future studies such as other PEG molecules, silane molecules or dextran in order to increase the internalization of iron to obtain values that can be detected using the thiocyanate- or ferrozine method. Some reports have indicated that coated nanoparticles are internalized in a lower degree compared to non-coated particles, and therefore further investigation of internalization of naked particles are of interest.

A large amount of cells was required in this study in order to obtain detectable amount of internalized iron. The cells can in future studies be cultured in wells with larger adhesion area, such as 6 well plates, for easier and less time consuming harvesting procedure. Parameters such as exposure time of nanoparticles can be changed as one publication has indicated that a maximum uptake was seen after 4 days of exposure to nanoparticles [26]. If internalization is further optimized, fewer cells could be used which would facilitate the procedure.

The method developed in this work can be used with other cell types such as THP-1 (human acute monocytic leukemia), RAW264 (mouse leukemic monocyte-macrophages), MDA-MB-436 (human breast adenocarcinoma) and JURKAT (T cell leukemia) to gain information of the interaction between IXG-P and other tumour cell types. Using the same methodology, the uptake of nanoparticles can also be studied in primary cell lines such as HUVEC (Human Umbilical Vein Endothelial Cells), HASMC (Human Aortic Smooth Muscle Cells) and HMEC (Human Mammary Epithelial Cells).

The knowledge gained from this study can be used for further development of the particle developed at Spago Imaging AB with respect to e.g. limiting the interaction with non-tumorous tissue and increasing tumour targeting.

References

1. Jokerst, J.V., et al., *Nanoparticle PEGylation for imaging and therapy.* Nanomedicine, 2011. 6(4): p. 715-728.
2. Zhu, X.-M., et al., *Enhanced cellular uptake of aminosilane-coated superparamagnetic iron oxide nanoparticles in mammalian cell lines.* International Journal of Nanomedicine, 2012. 7.
3. Freese, C., et al., *Size- and Coating-Dependent Uptake of Polymer-Coated Gold Nanoparticles in Primary Human Dermal Microvascular Endothelial Cells.* Biomacromolecules, 2012. 13(5): p. 1533-1543.
4. Sardanelli, F., et al., *Sensitivity of MRI versus mammography for detecting foci of multifocal, multicentric breast cancer in fatty and dense breasts using the whole-breast pathologic examination as a gold standard.* American Journal of Roentgenology, 2004. 183(4): p. 1149-1157.
5. Huang, B., M.W.-M. Law, and P.-L. Khong, *Whole-Body PET/CT Scanning: Estimation of Radiation Dose and Cancer Risk.* Radiology, 2009. 251(1): p. 166-174.
6. Berg, W.A., et al., *Detection of Breast Cancer With Addition of Annual Screening Ultrasound or a Single Screening MRI to Mammography in Women With Elevated Breast Cancer Risk.* Jama-Journal of the American Medical Association, 2012. 307(13): p. 1394-1404.
7. Stanford medicine, C.i. 2013; Available from: cancer.stanford.edu.
8. Joseph P. Hornak, P.D., *The Basics of MRI*. 1996, Rochester, N.Y. :Rochester Institute of Technology.
9. Lee, G.H., Y. Chang, and T.J. Kim, *Blood-Pool and Targeting MRI Contrast Agents: From Gd-Chelates to Gd-Nanoparticles.* European Journal of Inorganic Chemistry, 2012(12): p. 1924-1933.
10. Brown, M.A. and R.C. Semelka, *MRI: Basic Principles and Applications*. Vol. 4th ed. 2010: Wiley- Blackwell. 1-27.
11. Weinmann, H.J., et al., *Tissue-specific MR contrast agents.* European Journal of Radiology, 2003. 46(1).
12. Administration., U.S.F.a.D. *Important drug warning for gadolinium-based contrast agents.* 2007; Available from: http://www.fda.gov/downloads/Safety/MedWatch/SafetyInformation/SafetyAlertsforHumanMedicalProducts/UCM154532.pdf.
13. Tan, M., et al., *Synthesis and Evaluation of Nanoglobular Macrocyclic Mn(II) Chelate Conjugates as Non-Gadolinium(III) MRI Contrast Agents.* Bioconjugate Chemistry, 2011. 22(5).
14. AB, S.I. 2012 [cited 2013 2013-01-15]; Available from: www.spagoimaging.com.
15. Fang, J., H. Nakamura, and H. Maeda, *The EPR effect: Unique features of tumor blood vessels for drug delivery, factors involved, and limitations and augmentation of the effect.* Advanced Drug Delivery Reviews, 2011. 63(3): p. 136-151.
16. Hofmann-Amtenbrink, M., H. Hofmann, and X. Montet, *Superparamagnetic nanoparticles - a tool for early diagnostics.* Swiss Medical Weekly, 2010. 140.
17. Albanese, A. and W.C.W. Chan, *Effect of Gold Nanoparticle Aggregation on Cell Uptake and Toxicity.* Acs Nano, 2011. 5(7).
18. Murph, S.E.H., et al., *Manganese-gold nanoparticles as an MRI positive contrast agent in mesenchymal stem cell labeling.* Journal of Nanoparticle Research, 2012. 14(4).
19. Kresse, M., et al., *Targeting of ultrasmall superparamagnetic iron oxide (USPIO) particles to tumor cells in vivo by using transferrin receptor pathways.* Magnetic Resonance in Medicine, 1998. 40(2).
20. Elias, A. and A. Tsourkas, *Imaging circulating cells and lymphoid tissueswith iron oxide nanoparticles*. 2009, American Society of Hematology: Department of Bioengineering, University of Pennsylvania, Philadelphia. p. 720-726.

21. Lin, C., S. Cai, and J. Feng, *Positive Contrast Imaging of SPIO Nanoparticles.* Journal of Nanomaterials, 2012.
22. Daniel, M.C. and D. Astruc, *Gold nanoparticles: Assembly, supramolecular chemistry, quantum-size-related properties, and applications toward biology, catalysis, and nanotechnology.* Chemical Reviews, 2004. 104(1).
23. Arnida, A. Malugin, and H. Ghandehari, *Cellular uptake and toxicity of gold nanoparticles in prostate cancer cells: a comparative study of rods and spheres.* Journal of Applied Toxicology, 2010. 30(3).
24. Thorek, D.L.J., et al., *Superparamagnetic iron oxide nanoparticle probes for molecular imaging.* Annals of Biomedical Engineering, 2006. 34(1).
25. Gupta, A.K. and A.S.G. Curtis, *Surface modified superparamagnetic nanoparticles for drug delivery: Interaction studies with human fibroblasts in culture.* Journal of Materials Science-Materials in Medicine, 2004. 15(4).
26. Zhang, Y., N. Kohler, and M.Q. Zhang, *Surface modification of superparamagnetic magnetite nanoparticles and their intracellular uptake.* Biomaterials, 2002. 23(7): p. 1553-1561.
27. Chithrani, B.D. and W.C.W. Chan, *Elucidating the mechanism of cellular uptake and removal of protein-coated gold nanoparticles of different sizes and shapes.* Nano Letters, 2007. 7(6): p. 1542-1550.
28. Jin, H., et al., *Size-Dependent Cellular Uptake and Expulsion of Single-Walled Carbon Nanotubes: Single Particle Tracking and a Generic Uptake Model for Nanoparticles.* Acs Nano, 2009. 3(1): p. 149-158.
29. Iversen, T.-G., T. Skotland, and K. Sandvig, *Endocytosis and intracellular transport of nanoparticles: Present knowledge and need for future studies.* Nano Today, 2011. 6(2).
30. Gerets, H.H.J., et al., *Characterization of primary human hepatocytes, HepG2 cells, and HepaRG cells at the mRNA level and CYP activity in response to inducers and their predictivity for the detection of human hepatotoxins.* Cell Biology and Toxicology, 2012. 28(2): p. 69-87.
31. Kumar, M., et al., *Cellular interaction of folic acid conjugated superparamagnetic iron oxide nanoparticles and its use as contrast agent for targeted magnetic imaging of tumor cells.* International Journal of Nanomedicine, 2012. 7: p. 3503-3516.
32. Instruments, M., *Zeta sizer nano series*. Vol. Issue 1.0 june. 2003.
33. Anoopkumar-Dukie, S., et al., *Resazurin assay of radiation response in cultured cells.* British Journal of Radiology, 2005. 78(934): p. 945-947.
34. Walkey, C.D., et al., *Nanoparticle Size and Surface Chemistry Determine Serum Protein Adsorption and Macrophage Uptake.* Journal of the American Chemical Society, 2012. 134(4).
35. Chithrani, B.D., A.A. Ghazani, and W.C.W. Chan, *Determining the size and shape dependence of gold nanoparticle uptake into mammalian cells.* Nano Letters, 2006. 6(4): p. 662-668.
36. Woods, J.T. and M.G. Mellon, *Thiocyanate method for iron - A spectrophotometric study.* Industrial and Engineering Chemistry-Analytical Edition, 1941. 13: p. 0551-0554.
37. Viollier, E., et al., *The ferrozine method revisited: Fe(II)/Fe(III) determination in natural waters.* Applied Geochemistry, 2000. 15(6): p. 785-790.
38. Marsich, E., et al., *Biological response of hydrogels embedding gold nanoparticles.* Colloids and Surfaces B-Biointerfaces, 2011. 83(2): p. 331-339.
39. van Tiel, S.T., et al., *Variations in labeling protocol influence incorporation, distribution and retention of iron oxide nanoparticles into human umbilical vein endothelial cells.* Contrast Media & Molecular Imaging, 2010. 5(5).
40. Zhang, C., et al., *Silica- and alkoxysilane-coated ultrasmall superparamagnetic iron oxide particles: A promising tool to label cells for magnetic resonance imaging.* Langmuir, 2007. 23(3): p. 1427-1434.
41. Naseem, U., *Functionalized gold nanoparticles for specific genaration of oxidative stress*, in *Organic chemistry*. 2012, Lund University.
42. Fan, J.H., et al. *Biocompatibility Study of Gold Nanoparticles to Human Cells*. in *13th International Conference on Biomedical Engineering (ICBME)*. 2009. Singapore.

43. Matuszewski, L., et al., *Cell tagging with clinically approved iron oxides: Feasibility and effect of lipofection, particle size, and surface coating on labeling efficiency.* Radiology, 2005. 235(1).
44. Metz, S., et al., *Capacity of human monocytes to phagocytose approved iron oxide MR contrast agents in vitro.* European Radiology, 2004. 14(10).